PFAS in the water supply: source water contamination

Mussabek, Dauren

2021

Document Version:
Publisher's PDF, also known as Version of record

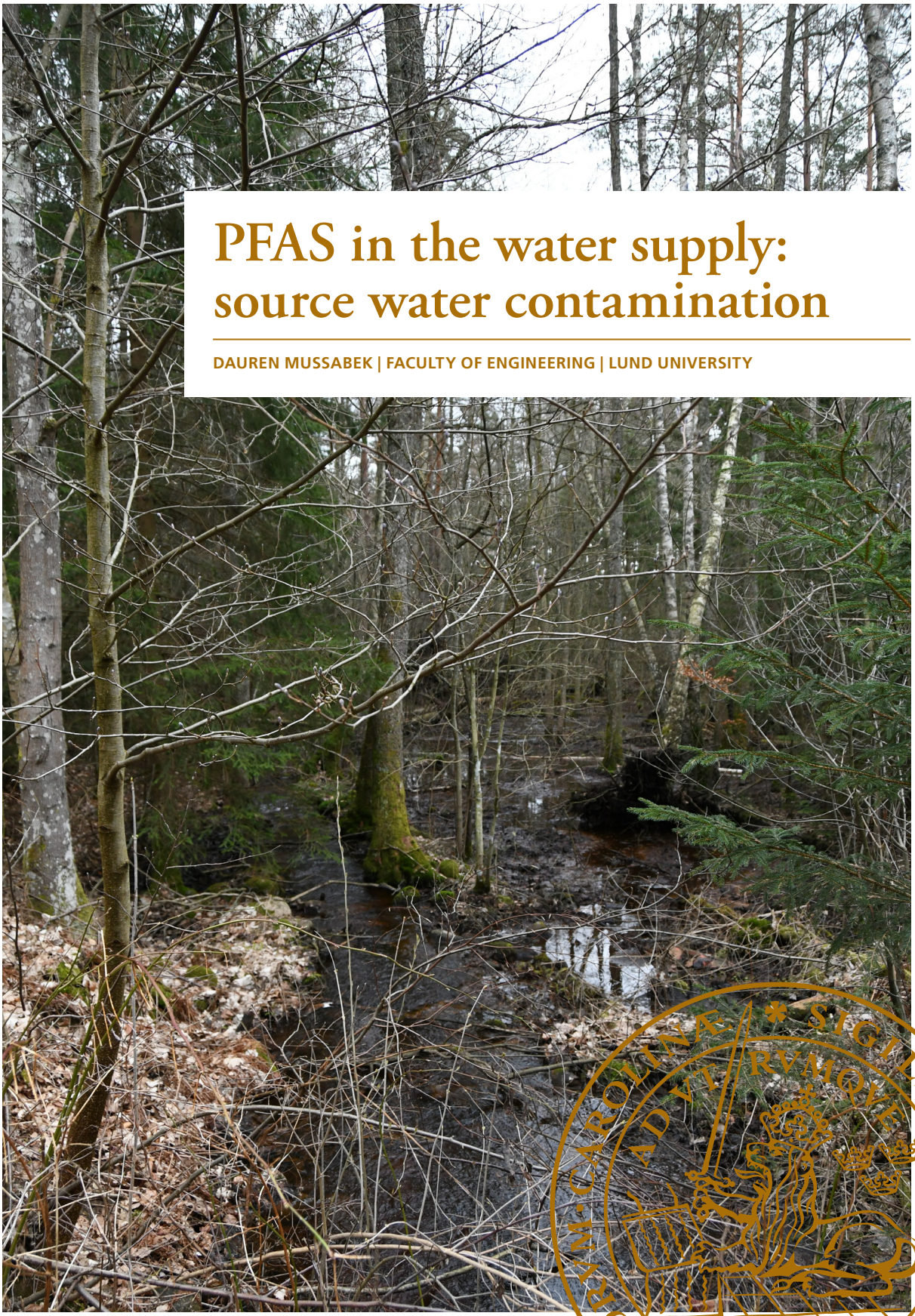

PFAS in the water supply: source water contamination

DAUREN MUSSABEK | FACULTY OF ENGINEERING | LUND UNIVERSITY

Printed by Media-Tryck, Lund 2021 NORDIC SWAN ECOLABEL 3041 0903

Lund University
Faculty of Engineering
Department of Building and Environmental Technology
Water Resources Engineering
ISBN 978-91-8039-020-0
ISSN 1101-9824
CODEN: LUTVDG/TVVR-1091 (2021)

PFAS in the water supply: source water contamination

Dauren Mussabek

LUND
UNIVERSITY

DOCTORAL DISSERTATION

by due permission of the Faculty of Engineering, Lund University, Sweden.
To be defended at Faculty of Engineering, V-building, John Ericssons Väg1,
Lund, room V:C on October 14, 2021 at 10.15 a.m.

Faculty opponent
Prof. Dr. Lars Rosén

Organization LUND UNIVERSITY Division of Water Resources Engineering PO Box 118, SE-221 00 Lund, Sweden Author: Dauren Mussabek	**Document name** Doctoral Thesis, report TVVR 1091 **Date of issue** 2021-09-18 Sponsoring organization

Title and subtitle
PFAS in the water supply: source water contamination

Abstract
Water contamination with per- and polyfluoroalkyl substances (PFAS) is a serious problem for water suppliers in many regions. Due to persistence of the substances and a complex distribution mechanism, PFAS can have an adverse impact on water quality. Reported toxicological and health effects, make it very important to minimise the of wildlife and human exposure to PFAS. The exposure path is, however, associated with the most vital resource as water.

Mitigation of the PFAS contamination is an extensive challenge that requires a multidisciplinary investigation of the pollution nature and distribution mechanisms in the aquatic environment. Furthermore, since conventional drinking water treatment is insufficient in PFAS removal, development of the treatment alternative is necessary. Not least due to substantial number of contaminated water sources and an increasing worldwide demand on drinking water.

Present thesis was built around investigation of the historical source water contamination and human exposure to PFAS at studied locations in Ronneby (primarily) and Luleå in Sweden. Several interconnected studies were conducted regarding present contamination levels, transport and distribution mechanism, contamination and emission history, as well as PFAS treatment alternatives for drinking water.

PFAS analysis and assessment of the contamination levels in surface water, groundwater, and sediments were conducted. PFAS occurrence at studied locations was connected to historical use of PFAS containing aqueous film forming foam (PFAS-AFFF). By means of core analysis, accumulation period was studied for the exposed recipient (Lake). Furthermore, influence of the media characteristics (i.e., mineral composition, density, moisture, and organic matter content) on PFAS distribution in sediment was studied and corresponding distribution (partitioning) predictors were estimated. Regarding emission source, profiling of the possible PFAS-AFFF compositions was conducted (based on groundwater analysis), and possible application and emission scenarios were evaluated (based on available fire-training history and related protocols). Investigation of PFAS treatment methods for drinking water was conducted and implementation of ex-situ treatment technique, based on UVC/VUV induced removal, was suggested. The laboratory scale treatment unit was developed and tested in series of experimental trials with PFCAs, PFSAs, FTSAs, and FASAs.

Key words: source water, drinking water, per- and polyfluoroalkyl substances, PFAS, AFFF, UV treatment

Classification system and/or index terms (if any)

Supplementary bibliographical information		**Language** English
ISSN and key title 1101-9824		**ISBN** 978-91-8039-020-0 (print) 978-91-8039-021-7 (pdf)
Recipient's notes	**Number of pages** 210	Price
	Security classification	

Signature  Date 2021-09-06

PFAS in the water supply: source water contamination

Dauren Mussabek

LUND
UNIVERSITY

Coverphoto by Dauren Mussabek

Faculty of Engineering
Department of Building and Environmental Technology
Division of Water Resources Engineering

ISBN 978-91-8039-020-0 (print)
978-91-8039-021-7 (pdf)
ISSN 1101-9824
Report TVVR 1091

Printed in Sweden by Media-Tryck, Lund University, Lund 2021

Another question is, How far should theory go in its analysis of the means? Evidently only so far as the elements in a separate form present themselves for consideration in practice.

Carl von Clausewitz

Table of Contents

Acknowledgements

I would like to thank the Lars Erik Lundberg Scholarship Foundation for supporting almost entire duration of my doctoral studies.

I would like to thank my supervisors Prof. Kenneth M. Persson and Prof. Ronny Benrndtsson for giving me the opportunity to pursue a doctoral degree and introducing me into the word of water and engineering. I would like to express my sincere gratitude for your encouragement, trust, and not least, for your great patience and support during my studies.

Many thanks to my co-supervisors: Assoc. Prof. Lutz Ahrens, for the dive into PFAS and analysis, guidance in field investigation, careful supervision and detailed attention to projects; Prof. Kei Nakagawa, for inspiration, help with work, useful suggestions on methods and interesting field experiences; and Prof. Magnus Persson, for the guidance in hydrogeology and transport aspects, as well as for friendly support in difficult moments.

I would like to thank Prof. Kristina Jakobsson and her group for having me in the project and providing me with various useful hints and suggestions throughout the course of my studies.

I would like to express my gratitude to Kent Broström and Mattias Andersson at Ronneby Miljö & Teknik AB for help with investigation and shared knowledge. Very little would be possible without your inputs and support.

Thanks to Prof. Lars Wadsö, for help and suggestions with sorption and transport processes; Assoc. Prof. Mats Rundgren, for giving me a whole new perspective on sediment and suggestions with radioisotope analysis; and Prof. Magnus Larsson, for interesting discussions, as well as for various useful books.

I would like to thank all my colleagues at TVRL. Thanks to Caroline Hallin for help with navigating the education process, finding tools and data sources.

Lastly, I would like to thank my friends and colleagues Laura Gobelius, Vera Franke and Tomomi Imura for timely help and support, interesting work and exciting time in the laboratory. Thanks to Han Yu for friendship, interesting life advices and help.

Abstract

Water contamination with per- and polyfluoroalkyl substances (PFAS) is a serious problem for water suppliers in many regions. Due to persistence of the substances and a complex distribution mechanism, PFAS can have an adverse impact on water quality. Reported toxicological and health effects, make it very important to minimise the of wildlife and human exposure to PFAS. The exposure path is, however, associated with the most vital resource as water.

Mitigation of the PFAS contamination is an extensive challenge that requires a multidisciplinary investigation of the pollution nature and distribution mechanisms in the aquatic environment. Furthermore, since conventional drinking water treatment is insufficient in PFAS removal, development of the treatment alternative is necessary. Not least due to substantial number of contaminated water sources and an increasing worldwide demand on drinking water.

Present thesis was built around investigation of the historical source water contamination and human exposure to PFAS at studied locations in Ronneby (primarily) and Luleå in Sweden. Several interconnected studies were conducted regarding present contamination levels, transport and distribution mechanism, contamination and emission history, as well as PFAS treatment alternatives for drinking water.

PFAS analysis and assessment of the contamination levels in surface water, groundwater, and sediments were conducted. PFAS occurrence at studied locations was connected to historical use of PFAS containing aqueous film forming foam (PFAS-AFFF). By means of the core analysis, accumulation period was studied for the exposed recipient (Lake). Furthermore, influence of the media characteristics (i.e., mineral composition, density, moisture, and organic matter content) on PFAS distribution in sediment was studied and corresponding distribution (partitioning) predictors were estimated. Regarding emission source, profiling of the possible PFAS-AFFF compositions was conducted (based on groundwater analysis), and possible application and emission scenarios were evaluated (based on available fire-training history and related protocols). Investigation of PFAS treatment methods for drinking water was conducted and implementation of ex-situ treatment technique, based on UVC/VUV induced removal, was suggested. The laboratory scale treatment unit was developed and tested in series of experimental trials with PFCAs, PFSAs, FTSAs, and FASAs.

Keywords: source water, drinking water, per- and polyfluoroalkyl substances, PFAS, AFFF, UV treatment

Popular science summary in Swedish

I denna avhandling har förekomst och spridning av PFAS (poly- och perfluorerade alkylsubstanser) från brandskum för släckning av fotogen- och bensinbränder undersökts i Kallinge och Kallax i Sverige. Vidare har transport av PFAS-föroreningar modellerats i ytvatten och grundvatten från brandövningsplatsen i Kallinge till grundvattenmagasinet och Ronneby Miljö och Tekniks vattenverk Brantafors i Kallinge. Slutligen har en metod för avancerad oxidation av PFAS med hjälp av kortvågig ultraviolett strålning tagits fram för att undersöka om det går att bryta ned PFAS till kortare organiska molekyler som lättare kan brytas ner.

PFAS är ett samlingsnamn för en stor grupp ämnen som började användas i mitten av 1900-talet då de har en mängd intressanta tekniska egenskaper som låg vattenlöslighet, hög temperaturstabilitet som används för släta vatten-, fett- och smutsavvisande ytor. De återfinns i impregnerade textilier, impregnerat papper, rengöringsmedel och brandsläckningsskum och används i bland annat verkstads- och elektronikindustrin. Det finns över 4000 olika ämnen i PFAS-gruppen. De mest kända substanserna är PFOS (perfluoroktansulfonat) och PFOA (perfluoroktansyra). De tekniskt viktiga egenskaperna betyder även att många PFAS-ämnen är hälsofarliga och svårnedbrytbara, bioackumulerbara och ofta ytaktiva.

Miljöproblem med PFAS började uppmärksammas alltmer från slutet av 1990-talet. EU beslöt att förbjuda PFOS och förbjöd försäljning från juni 2007, men det var tillåtet att använda släckskum fram till juni 2011. Det är praxis att marknaden får ett par år att anpassa sig till de nya reglerna men fyra års utfasning är en ganska lång tid.

Brandskum används ofta för att släcka bränder med snabba förlopp, t ex bränder i bränsletankar på flygplan. Vid svenska flygflottiljer har brandövningar med PFAS-haltigt brandskum genomförts åtminstone sedan sent 1980-tal. I avhandlingen detaljstuderas ytvatten och grundvatten nedströms brandövningsplattorna vid Norrbottens Flygflottilj F21 i Kallax och Blekinge Flygflottilj F17 i Kallinge.

Bägge ligger nära grundvattentäkter som användes för dricksvattenförsörjning. Mätningarna visar att en plym med PFAS-föroreningar rör sig från brandövningsplatserna till grundvattenmagasinen. Länsstyrelsen i Blekinge valde vid en miljöskanning av dricksvatten i länet 2013 att ta prover på dricksvattentäkten i Kallinge. Nivåerna av PFAS var kraftigt förhöjda och mycket högre än vad som uppmätts någon annanstans i Sverige. Ronneby kommuns vattenbolag tog prover som bekräftade mycket höga PFAS-halter och vattentäkten stängdes omedelbart den 16 december 2013.

I Kallax uppmättes PFAS-halter motsvarande 1700 ng/l som högst. Ungefär 70% av ämnena var olika svavelhaltiga PFAS-föreningar, medan knappt 30% var PFAS som

innehöll karboxylgrupper. I sjösediment nedströms brandövningsplatsen gick det att följa hur långt ned PFAS-ämnen hunnit läcka.

I Kallinge var halterna ungefär tio gånger högre än i Kallax och även i ytvatten i dammar vid övningsplatsen kunde halter kring 100 ng/l uppmätas. Vid undersökningar av sedimentets innehåll av oorganiskt material kunde en tydlig koppling mellan det oorganiska innehållet och förhöjda PFAS-halter registreras, medan den organiska fraktionen inte verkade direkt påverka anrikning av PFAS i sedimenten.

En simuleringsstudie genomfördes för Kallinge för att klargöra när i tiden PFAS-användningen på brandövningsplatsen kunde tänkas ha inletts. Modell-beräkningarna tyder på att mellan 1 och 44 kg PFAS -ämnen kan frigöras per enskild övning på brandövningsplatsen. Övningarna har bedrivits i minst 25 år.

Rening med hjälp av ultraviolett (UVC/VUV) ljusbehandling verkar bryta upp framför allt bindningen mellan svavelföreningen och kolkedjan i PFAS respektive bindningen mellan karboxylgruppen och kolkedjan. Men om UV-ljuset får verka på vattnet under tillräckligt lång tid börjar också delar av kolkedjan att brytas upp. Reaktionshastigheten är oberoende av ursprungshalten i vattnet.

List of publications

This thesis is submitted with the support of the following papers, which are referred by Roman numerals in the text body.

Appended papers

I Dauren Mussabek, Lutz Ahrens, Kenneth M. Persson, and Ronny Berndtsson, Temporal trends and sediment-water partitioning of per- and polyfluoroalkyl substances (PFAS) in lake sediment, Chemosphere 2019, 227, 624-629.

II Dauren Mussabek, Kenneth M. Persson, Ronny Berndtsson, Lutz Ahrens, Kei Nakagawa, and Tomomi Imura, Impact of the Sediment Organic vs. Mineral Content on Distribution of the Per- and Polyfluoroalkyl Substances (PFAS) in Lake Sediment, Int. J. Environ. Res. Public Health 2020, 17, 5642.

III Dauren Mussabek, Kenneth M Persson, Ronny Berndtsson, and Lutz Ahrens Historical groundwater contamination with PFAS: addressing the emission source, Manuscript by authors, 2021.

IV Dauren Mussabek, Kenneth M Persson, Lutz Ahrens, Vera Franke, and Ronny Berndtsson, UVC/VUV induced treatment of PFAS in aqueous phase: removal of PFCAs, PFSAs, FTSAs and FASAs class representatives, Manuscript by authors, 2021.

Author's contribution to appended papers

I The author contributed to: conceptualization, development of methodology, and validation; conducted: investigation, formal analysis and writing of the original draft.

II The author conducted: conceptualization, design of methodology, investigation, formal analysis, validation and writing of the original draft.

III The author conducted: conceptualization, design of methodology, investigation, formal analysis, validation and writing of the original draft.

IV The author conducted: conceptualization, design of methodology, investigation, formal analysis, validation and writing of the original draft.

Abbreviations and technical terms

AFFF	Aqueous film-forming foams	
AIX	Anion exchange (resins)	
CMC	Critical micellar concentration	
CRS	Constant rate of supply	
ECF	Electrochemical fluorination	
FAB-MS	Fast atom bombardment mass spectrometry	
GAC	Granular activated carbon	
HLB	Hydrophilic-lipophilic balance	
HPLC	High-performance liquid chromatography	
HRMS	High resolution mass spectrometry	
MS/MS	Tandem mass spectrometry	
NF	Nano filtration	
PFAS	Perfluoroalkyl and polyfluoroalkyl substances	
FASAs	Perfluoroalkane sulfonamides	
	FOSA	Perfluorooctane sulfonamide
	EtFOSA	N-Ethyl perfluorooctane sulfonamide
	MeFOSA	N-Methyl perfluorooctane sulfonamide
FOSAAs	Perfluoroalkane sulfonamido- acetic acids	
	FOSAA	Perfluorooctane sulfonamidoacetic acid
	EtFOSAA	N-Ethyl perfluorooctane sulfonamidoacetic acid
	MeFOSAA	N-Methyl perfluorooctane sulfonamidoacetic acid
FASEs	Perfluoroalkane sulfonamidoethanols	
	MeFOSE	N-Methyl perfluorooctane sulfonamidoethanol
	EtFOSE	N-Ethyl perfluorooctane sulfonamidoethanol
FTSAs	Fluorotelomer sulfonic acids	
	x:2 FTSA	x:2 Fluorotelomer sulfonic acid

PFCAs	Perfluoroalkyl carboxylic acids	
	PFBA	Perfluorobutanoic acid
	PFPeA	Perfluoropentanoic acid
	PFHpA	Perfluoroheptanoic acid
	PFHxA	Perfluorohexanoic acid
	PFOA	Perfluorooctanoic acid
	PFNA	Perfluorononanoic acid
	PFDA	Perfluorodecanoic acid
	PFUnDA	Perfluoroundadecanoic acid
	PFDoDA	Perfluorododadecanoic acid
	PFTriDA	Perfluorotridadecanoic acid
	PFTeDA	Perfluorotetradecanoic acid
	PFHxDA	Perfluorohexadecanoic acid
	PFOcDA	Perfluorooctadecanoic acid
PFSAs	Perfluoroalkane sulfonic acids	
	PFBS	Perfluorobutane sulfonic acid
	PFHpS	Perfluoroheptane sulfonic acid
	PFHxS	Perfluorohexane sulfonic acid
	PFOS	Perfluorooctane sulfonic acid
	PFDS	Perfluorooctane sulfonic acid
PFAS-AFFF	PFAS containing aqueous film-forming foams	
POCIS	Polar organic chemical integrative sampler	
TOF	Total organic fluorine (analysis)	
TOP	Total oxidable precursors (assay)	
UPLC	Ultra-performance liquid chromatography	
UV	Ultraviolet	
	UVC	Short-wave UV (200–280 nm)
	VUV	Vacuum UV (100–200 nm)
WAX	Weak anion-exchange	
XRF	X-ray fluorescence (analysis)	

Introduction

Purpose of the work; questions

The aim of the conducted research was to investigate the source water contamination with per- and polyfluoroalkyl substances (PFAS) and human exposure via drinking water. Corresponding studies were conducted at two sites affected by historical use of PFAS containing aqueous film forming foam (PFAS-AFFF) in Luleå (backup site) and Ronneby (primary site) in Sweden. These included: PFAS analysis and assessment of the present water contamination levels; analysis of the contaminant transport and distribution mechanism; investigation of the emission and contamination history; and analysis of the drinking water treatment, processing, and contamination (Figure 1).

Analysis of the water contamination with PFAS requires understanding of the cluster of interconnected processes and mechanisms. It is important to establish the contamination source and find the connection between PFAS-AFFF application and PFAS emission rates. Furthermore, since sorption and transport processes in the natural heterogeneous media are very complex, PFAS distribution in the aquatic environment, is yet subject to investigation. PFAS distribution is affected by both medium related features and contaminant behaviour in the dissolved state. Thus, objectives of the conducted research included improved understanding of how the fire-training and PFAS-AFFF application contributed to the PFAS emission; what effect does surfactant nature of PFAS have on distribution and transport in the aquatic environment; and not least, how can the source water contamination be addressed in a historical context.

Furthermore, it was necessary to improve the understanding of impact of the historical source water (groundwater) contamination on the drinking water quality. This meant to study the operation (water treatment and production) of the waterworks (Ronneby) and find a connection between variation in the PFAS level in source water and contamination level in supplied drinking water. Moreover, concerning the contaminant behaviour in drinking water production, it was important to study the treatment barrier efficiencies of those implemented at the waterworks (Ronneby), as well as in conventional water treatment plants.

Considering the drinking water treatment challenges associated with PFAS, it was important to study the ex-situ treatment alternatives. Thus, a design of UVC/VUV

treatment unit is suggested and tested. It was necessary to investigate the method performance and understand whether the suggested method is suitable for water treatment and operation at larger scales.

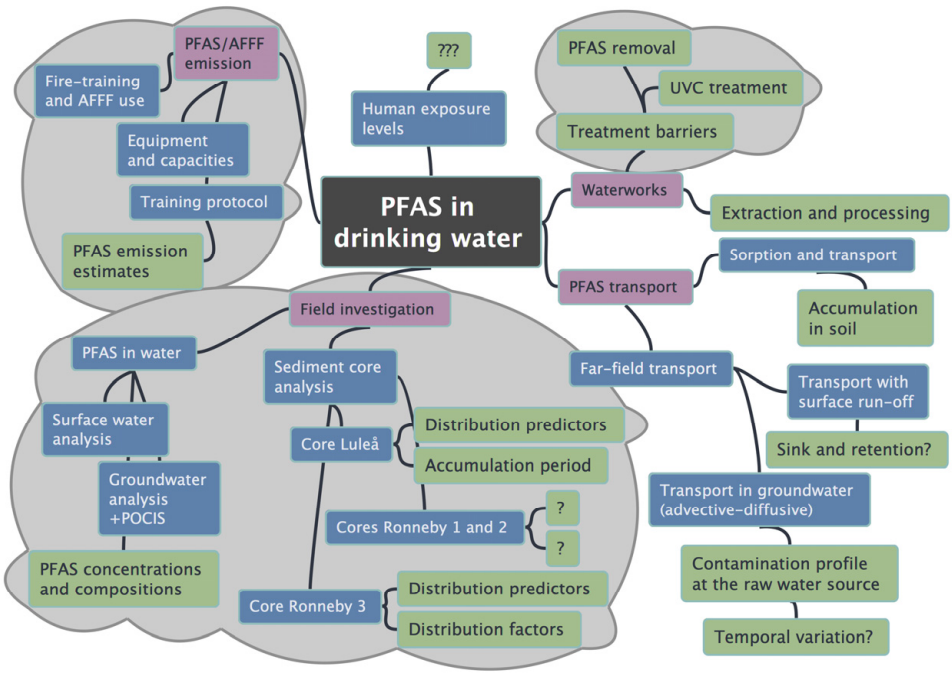

Figure 1. The methodological framework including corresponding studies (purple), sub-projects (blue), and expected outcomes (green) of the conducted research. Gray clouds represent the studies and outcomes that are appended and discussed in the present thesis.

However, due to the complexity of the involved processes, difficulties with method development and implementation, analytical challenges, and not least, the data limitations and restrictions, it was not possible to fully cover all important aspects. Therefore, in the present thesis, as well as in appended papers, the research objectives and outcomes are covered partially (Figure 1). Thus, the overall objective of the thesis work can be accordingly specified and addressed in the following research questions:

- How are the measured PFAS concentrations in water samples representative in relation to the emission source and overall contamination of the aquatic environment (Papers I, II, and III)?
- How can the timeframe of a historical contamination be established? Is the core analysis a representative approach (Papers I and II)?

- Are field-derived distribution predictors representative of overall transport phenomena? What factors can be affecting the PFAS distribution and behaviour (Papers I and II)?
- What do we need to know about PFAS emission source and what can investigation of the AFFF application history tell us (Paper III)?
- Can the far-field transport conditions and rates be addressed with limited prior knowledge (Paper III)?
- How can PFAS contaminated water be treated? Is UVC/VUV treatment method suitable for PFAS treatment and what PFAS classes are sensitive to this treatment (Paper IV)?

Background

PFAS

Perfluoroalkyl and polyfluoroalkyl substances (PFAS) represent a group of fluorinated surfactants (Figure 2) widely used in various industrial and commercial applications since the 1950s (Armitage et al., 2006; Prevedouros et al., 2006; Buck et al., 2011). The advantage of PFAS application is primarily connected to the remarkable thermal and chemical stability, which are inaccessible for most of the hydrocarbon-based surfactants (Kissa, 2001). PFCAs and PFSAs are persistent, without significant decomposition at high temperatures (<400°C) (Kauck and Diesslin, 1951; Kissa, 2001). The carbon-fluoride bond, the key feature of the fluorocarbon hydrophobe, is stable to acids, alkali, and oxidation (Kissa, 2001). Another key property of PFAS is associated with the surfactant integration in immiscible phase systems (i.e., adsorption in air-liquid, liquid-liquid, and solid-liquid interfaces). Fluorinated PFAS hydrophobe lowers the surfactant critical micellar concentration (CMC), giving the PFAS ability to lower the surface tension (in water) (to 20–30 mN m^{-1}) at significantly low concentrations (100–200 ppm). Based on empirical data, as a general rule, CMC of PFAS is approximately equal to CMC of hydrocarbon surfactants with a hydrocarbon chain 1.5 to 1.7 times longer that fluorocarbon chain (Shinoda et al., 1972; Kissa, 2001).

PFAS synthesis is primarily connected with two manufacturing processes, as electrochemical fluorination (ECF) and telomerization. Understanding of these production processes is of importance for interpretation of the PFAS occurrence and site specific PFAS composition (in relation to source) (Buck et al., 2011). In ECF, hydrogen atoms of an organic raw material are replaced by fluoride atoms during the electrolysis process conducted with anhydrous hydrogenfluoride (Alsmeyer et al., 1994; Buck et al., 2011). The ECF process results in production of the various

functional raw material including $C_8F_{17}SO_2F$ and $C_7F_{15}COF$ (major PFOS and PFOA material), sulfonamides (FASAs), and sulfonamido alcohols (FASEs) (Buck et al., 2011). The ETF process is often characterised by production of branched perfluorinated isomers (due to the free-radical nature of the process) alongside with expected linear isomers. A fraction of the branched isomers depends on the ECF process and conditions and can constitute up to 20-30% (in case with PFOA and PFAS) of the produced mixture of linear and branched isomers (Reagen et al., 2007; Buck et al., 2011).

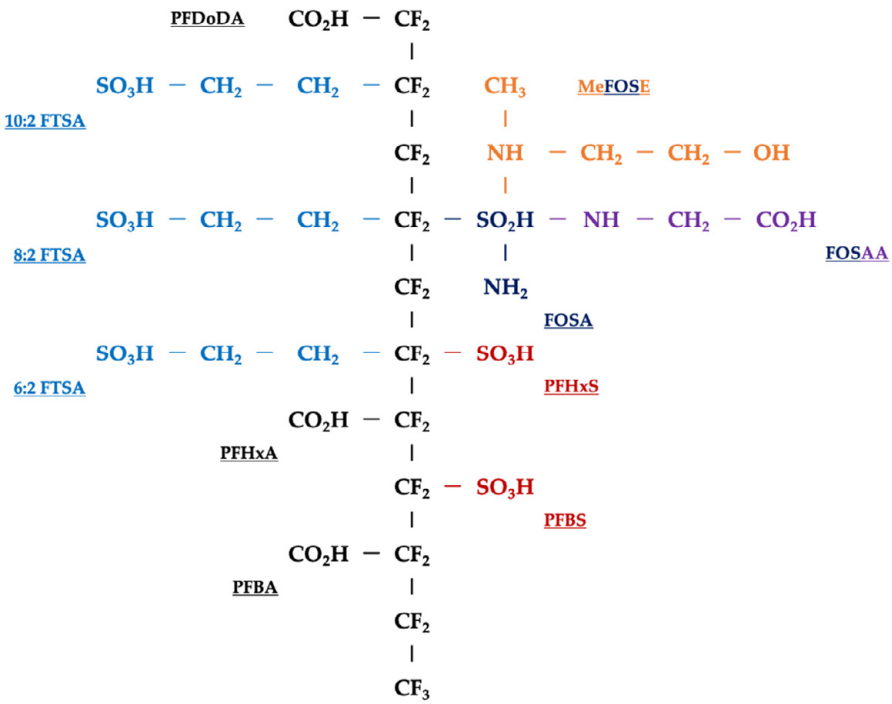

Figure 2. PFAS-tree representing the surfactant structure (fluorinated hyrophobe and hydrophile (functional group) of the four main class representatives PFCAs (PFBA, PFHxA and PFDoDA), PFSAs (PFBS and PFHxS), FTSAs (6:2 FTSA, 8:2 FTSA and 10:2 FTSA), and FOSAs (FOSA, FOSAA and MeFOSE)); compiled and schematised according to PFAS classification by Buck et al. (2011).

In the telomerisation process perfluoroalkyl iodide (PFAI) (i.e., C_2F_5I (PFEI)) reacts with tetrafluoroethylene ($C_2F_2{=}C_2F_2$ (TFE)) to consequently produce PFAI with longer perfluorinated chains ($C_mF_{2m+1}(CF_2CF_2)_nI$, telomer A) (Buck et al., 2011). Telomer A can further react to $C_mF_{2m+1}(CF_2CF_2)_nCH_2CH_2I$ (n:2 Fluorotelomer iodine (FTI), telomer B). Telomer A and B are the major functional material intermediates used for further production (Buck et al., 2011).

PFAS application includes a range of uses such as metal plating, surface repellents (textile, paper, and antifogging), coating formulations (i.e., paint, varnish, and inks), plastic, resin and rubber (PTFE and PVDF), oil industry, electronics (components and materials), semiconductors (photolithography and etching), cosmetics and personal care (emulsifiers, lubricants, and oleophobic agents), industrial and household cleaning products, and fire-fighting foams (as a surfactants in PFAS-AFFF) (Kissa, 2001; Armitage et al., 2006; Prevedouros et al., 2006; Paul et al., 2009; Jensen, 2010).

Firefighting foams and PFAS

The firefighting foam was first introduced in 1904 by Aleksandr Loran, as the fire protection measure superior to suppression with water. Technologies used in formulations, as well as in application, of the firefighting foams have since been evolving towards improved efficiency and handling (Rupert et al., 2005; Turekova and Karol, 2010). Modern firefighting foams are classified in several types depending on application purpose, handling standards, and equipment specifications (i.e., aqueous film forming foam (AFFF), alcohol-resistant AFFF, protein foams, alcohol resistant protein foams, fluoroprotein foams, class A foams, medium and high expansion foams, etc.). Commercially available foams are normally distributed as a concentrate (stock solution) ready for further dilution (as a foam solution) and foam aggregation (Rupert et al., 2005).

Firefighting foams are primarily used in fixed facility systems and emergency fire-rescue equipment. All firefighting foams have a certain hazardous impact on aquatic environment. This includes environmental impacts due to foam specific properties such as foaming, aquatic toxicity, oxygen demand and biodegradability, bioaccumulation, and oil emulsification. The general formulation of the firefighting foam concentrates includes water (<65%), solvents (<16%), surfactants (<17%), and other ingredients (<2%) (i.e., corrosion inhibitors, preservatives, dyes, etc). Commonly used surfactants include alkyl polyglycoside, alkyl dimethylamine oxides, octylphenoxypolyethoxyethanol, protein hydrolysate, benzotriazole, octanol sodium sulfate, PFAS, and more (Rupert et al., 2005).

PFAS introduction as surfactant in AFFF development was reported in the early 1960s (Kleiner and Jho, 2009; Cousins et al., 2016). Formulation of the PFAS containing Aqueous Film Forming Foam (PFAS-AFFF) has since been undergoing modification resulting in development of the PFAS based AFFF class (Rupert et al., 2005; Place and Field, 2012). Due to superior characteristics of PFAS as a surfactant, as well as the thermal stability, PFAS-AFFF found wide application in extinguishing hydrocarbon-fuel fires (Gramstad and Haszeldine, 1957; Kissa, 2001; Cousins et al., 2016). Following its early application in aircraft crash fire (3M Light Water at Los Angeles International Airport in 1978 (Kleiner and Jho, 2009), PFAS-

AFFF became an effective and perhaps a universal fire safety solution at the airfields worldwide (Cousins et al., 2016).

Environmental impacts

In certain cases, when emission of the utilized products is not confined, application of PFAS-AFFF can lead to contamination of the surrounding aquatic environment (as first reported in the late 1990s) (Levine et al., 1998; Moody and Field, 1999). The ubiquitous occurrence of PFAS in the proximity to firefighting training locations has been reported in many studies worldwide (Moody et al., 2002; Awad et al., 2011; Kärrman et al., 2011; Kwadijk et al., 2014). PFAS contamination can be connected to fire-training activities, firefighting equipment tests, as well as emergency events, where PFAS-AFFF application took place (Moody et al., 2002; Schultz et al., 2004; Weiss et al., 2012; Backe et al., 2013).

The occurrence of PFAS has been discussed in a wide range of environmental contexts (Houde et al., 2006; Ahrens and Bundschuh, 2014; Ahrens et al., 2015). PFAS have been detected in environmental matrices such as water, sediment, soil, and biota (Giesy and Kannan, 2001; Taniyasu et al., 2003; Houde et al., 2006; Pistocchi, 2009; Sakurai et al., 2010). Contamination of the aquatic environment and risks associated far-field transport are often connected to mobility of the substances in the dissolved phase and persistence to degradation under natural conditions (Filipovic et al., 2015b; McCarthy et al., 2017b). The environmental distribution of PFAS have been studied at both global and local scale (Armitage et al., 2006; Prevedouros et al., 2006; Sakurai et al., 2010). The spread of contaminants in water has been shown to have impact on wildlife (Taniyasu et al., 2003; Houde et al., 2006; Armitage et al., 2009; Greaves and Letcher, 2013). PFAS are considered toxic and associated with accumulation in living tissue (Andersen et al., 2008; Houde et al., 2008).

After release from the source area, PFAS can be accumulated and/or distributed in the surface water (Ahrens et al., 2015), sediment, soil (Ahrens et al., 2011; Zareitalabad et al., 2013), and groundwater (Moody et al., 2003; Filipovic et al., 2015b; Weber et al., 2017). For localized sources, in particular airfields, PFAS emission can contribute to a historical contamination of the water (Filipovic et al., 2015b; Hu et al., 2016; Andersson et al., 2019; Ryota, 2019; Li et al., 2020).

PFAS contamination of the source water can lead to human exposure via drinking water (Shin et al., 2013; Andersson et al., 2019; Ryota, 2019). There are several serious human exposure cases reported and PFAS have been subjected to a range of negative and potentially adverse health effects (Kerger et al., 2011; Shin et al., 2013; Mastrantonio et al., 2018; Oberg et al., 2018; Andersson et al., 2019).

Far-field transport of PFAS has been studied in surface water (Filipovic et al., 2013; Filipovic et al., 2015a) and groundwater (Shin et al., 2014; Weber et al., 2017).

PFAS circulation in the urban (and/or industrial) water and waste handling cycles has been connected to the occurrence at water treatment plants (Sinclair and Kannan, 2006; Gobelius et al., 2019) and landfills (Busch et al., 2010). However, interpretation of transport conditions, requires further investigation. Due to the surfactant nature of PFAS and complex distribution processes in the corresponding domain, a better understanding of the contaminant interaction in carrier phase–media interface is necessary (Jeon et al., 2011; Hellsing et al., 2016; Nouhi et al., 2018; Pereira et al., 2018). Moreover, PFAS distribution can be affected by certain macroscopic conditions related to environmental features of the area and emission source. This contributes to a large variation in the field-derived distribution predictors for PFAS (Zareitalabad et al., 2013; McCarthy et al., 2017b; Weber et al., 2017). PFAS sorption and transport processes in natural systems are yet subject for investigation.

Analysis and interpretation of the water contamination with PFAS require understanding of a cluster of interconnected processes, including analysis of the contamination levels, spatial distribution, as well as contamination history. In contamination linked to PFAS-AFFF application, application scenarios, used equipment, and purpose of the application play a significant role in PFAS distribution, contamination levels, and composition. PFAS-AFFF application can be relatively continuous or related to an emergency event, thus affecting the consequent contamination distribution (Awad et al., 2011; Filipovic et al., 2015b). It is often not known how often, under which conditions or with which chemical speciation PFAS-AFFF has been practised. Further investigations are important for better understanding of the water contamination by PFAS, and related distribution processes, also taking uncertainties into account.

Mitigation and treatment

Development of PFAS mitigation strategies and treatment prospects has become important during the last decade (Rahman et al., 2014; Dickenson and Higgins, 2016; Kucharzyk et al., 2017). PFAS removal has been studied in full-scale water treatment plants and systems (Quinones and Snyder, 2009; Appleman et al., 2014; Dickenson and Higgins, 2016; Gobelius et al., 2019). However, evaluation of conventional water treatment barriers, including physical separation and coagulation, aeration, filtration, and disinfection, has shown considerably low removal rates (Appleman et al., 2014; Kucharzyk et al., 2017; Gobelius et al., 2019).

From the existing treatment approaches, sorption on granular activated carbon (GAC) has been found suitable for PFAS treatment (Ochoa-Herrera et al., 2008; Kucharzyk et al., 2017). Although, adjustment to operation cycles, thermal incineration, and recombination of GAC can represent a big operational and maintenance challenge for the water suppliers (Rayne and Forest, 2009; Franke et al., 2021). In absence of alternatives, PFAS removal in sorption processes has been

considered economically and operationally superior to existing oxidation and separation techniques (Rayne and Forest, 2009; Kucharzyk et al., 2017). Furthermore, modification of the sorbent material and replacement alternatives has been considered (Deng et al., 2015). In removal using GAC, the PFAS treatment processes can be influenced by grain size and PFAS saturation levels in connection to the molecular chain-length (Rayne and Forest, 2009; Espan et al., 2015; Dickenson and Higgins, 2016). Considering the operational challenges related to PFAS removal, there is a great need for further investigation and development of ex-situ treatment methods and combinations.

Various alternative approaches have been suggested, including biological degradation, filtration, thermal destruction, and advanced oxidation methods. Microbial PFAS degradation (Schroder, 2003) and fungal degradation (Colosi et al., 2009) have shown a certain reduction potential. PFAS decomposition by microorganisms is linked to potential ingestion of the compounds (Colosi et al., 2009). However, persistence to oxidation under natural conditions, associated with fluoride-saturation of the carbon chain, makes PFAS insufficient for utilisation as energy source (Colosi et al., 2009). Observed reduction can possibly be associated with the bulk sorption process (Schroder, 2003) and further investigation is necessary for validation of the removal mechanisms (Merino et al., 2016; Kucharzyk et al., 2017).

Particular attention has been given to filtration techniques including microfiltration, nanofiltration, reverse osmosis, and combinations with other techniques (Dickenson and Higgins, 2016; Soriano et al., 2017; Franke et al., 2019). Although, microfiltration is theoretically inefficient for PFAS removal, it can be used in combination with prior separation using sorption (Franke et al., 2019; Murray et al., 2019; Franke et al., 2021). Nanofiltration and reverse osmosis and/or different combinations have shown considerable PFAS separation of >98% even for short-chain PFAS like PFBA (Dickenson and Higgins, 2016). Membrane techniques are straightforward in operation and the membranes themselves have long life-times if operated correctly. However post-process treatment or storage is required for the reject water resulting from nanofiltration or reverse osmosis (Franke et al., 2021).

PFAS degradation techniques have been tested with a range of physical processes. These, include pyrolytic decomposition (induced by sonochemical treatment) (Vecitis et al., 2008a; Rayne and Forest, 2009; Vecitis et al., 2010) and electrochemical treatment (tested for different anode/cathode, and counter electrode configurations) (Carter and Farrell, 2008; Ochiai et al., 2011a; Ochiai et al., 2011b; Ochiai et al., 2011c; Schaefer et al., 2015). Upscaling considerations have been made for sonochemical treatment (Vecitis et al., 2008a; Vecitis et al., 2008b; Vecitis et al., 2010). For electrochemical treatment, however, a precaution of transformation by-products is necessary (Trautmann et al., 2015; Merino et al., 2016; Schaefer et al., 2017). Advanced oxidation processes have been reported suitable for PFAS treatment, and often proposed in combination with prior treatment/separation

processes (Rayne and Forest, 2009; Espan et al., 2015; Kucharzyk et al., 2017). Implementation of advanced oxidation methods in PFAS treatment is mainly connected to high oxidation potential that is not accessible in biological and classical physicochemical treatment approaches (Schroder and Meesters, 2005; Merino et al., 2016). PFAS decomposition induced by strongly oxidising radical species has been reported with application of ozone, ultraviolet, hydrogen peroxide, ferrous ions, and their combinations (Schroder and Meesters, 2005; Espan et al., 2015; Dombrowski et al., 2018). However, further investigation regarding application of the advanced oxidation methods is needed.

Ultraviolet induced degradation in aqueous state has been reported applicable for PFAS treatment. There are different approaches and combinations with catalysis and other processes. However, limited attention has been given to UV exposure conditions (Giri et al., 2012). Furthermore, the PFAS removal efficiency is often assessed from limited PFAS inventory (Merino et al., 2016; Kucharzyk et al., 2017). Further investigation is necessary regarding the application of UV induced treatment of PFAS, and efficiency on a wide range of substances represented by the PFAS family.

PFAS in drinking water

There are still no parametric values for PFAS in drinking water in Sweden. Since 2014, the Swedish Food Agency (Livsmedelsverket) has been suggesting >90 ng L^{-1} as ΣPFAS concentration, when actions are needed to be taken ("åtgärdsnivå"). This recommendation was initially defining the limit of >90 ng L^{-1} for 7 PFAS (i.e., PFPeA, PFHxA, PFHpA, PFOA, PFBS, PFHxS and PFOS). Later in 2016, recommended limit was extended to 11 PFAS (i.e., PFBA, PFPeA, PFHxA, PFHpA, PFOA, PFNA, PFDA, PFBS, PFHxS, PFOS and 6:2 FTSA). In practice, ΣPFAS concentration <90 ng L^{-1} has been permissible since 2014 (Livsmedelsverket, 2021).

The EU Drinking Water Directive (2020/2184) has set the limit for ΣPFAS concentration in drinking water to 100 ng L^{-1} (for 20 PFAS) and 500 ng L^{-1} (for total PFAS) in 2020 (EU, 2020). Considering the ubiquitous occurrence of PFAS in water sources, and due to the fact, that drinking water is one of the most contributing food categories among the age groups, a tolerable weekly intake (TWI) threshold of 4.4 ng kg^{-1} (of body weight) per week was set by European Food Safety Authority (EFSA) in 2020 (EFSA, 2020). This would mean, that for an average healthy person permissible ΣPFAS concentration in drinking water must be <30–40 ng L^{-1}.

Materials and Methods

Field investigations

Study sites

Field investigations were conducted at sites in Luleå (Paper I) and Ronneby (Paper II and III) in Sweden. Water contamination with PFAS has been reported at both studied locations. PFAS contamination is primary connected to emission with PFAS-AFFF during fire-training activities and firefighting equipment tests.

In Luleå (Paper I), two water bodies were investigated: L (lake) and P (pond), both located approximately 500 m south-west of a firefighting training facility at the Norrbotten Air Force Wing (F21) (Figure 3).

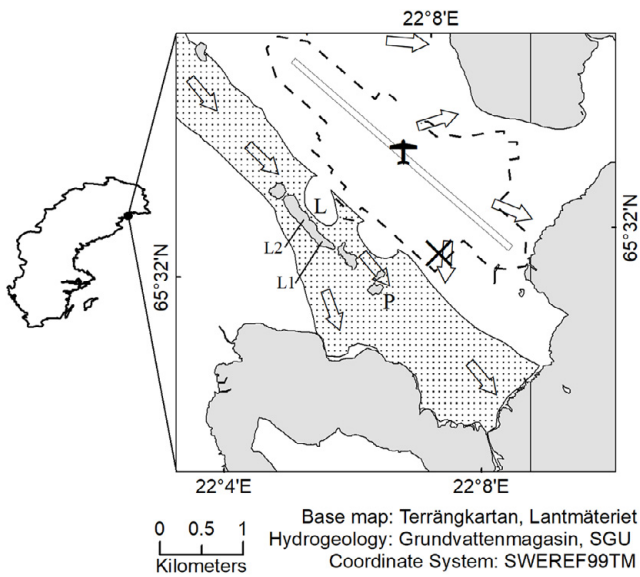

Figure 3. Sampling locations L (lake), P (pond) and L1 and L2 (sediment cores); dashed line defines the airport (F21, Luleå, Sweden) area; the cross indicates the fire training facility; dotted area defines the groundwater reservoir and the arrows show the groundwater flow direction (Figure 1 in Paper I).

F21 holds the largest flight exercise area in Sweden and has been active since 1941. The firefighting training facility at F21 has utilized PFAS-containing AFFFs during the last decades. The sampling site is located in a subarctic climate area with annual average temperature of 2°C and annual average precipitation of about 500 mm (SMHI, 2019).

The lake L (65°31'N, 22°5'E) is oligotrophic with an average depth of 13 m and surface area of about 0.1 km^2. Both the lake L and pond P (65º31'25"N, 22º6'28"E) were formed on an old gravel/sand pit (artificially excavated). The lake L (and pond P) are laying above a groundwater reservoir with high-permeable soil (glaciofluvial deposits). The sampling locations (lake L and pond P) were considered as receiving water bodies that can potentially impact the groundwater quality. Due to climatic conditions (soil saturation and extensive seasonal runoff (Bengtsson and Westerstrom, 1992), the transport with surface runoff is suggestively indicated as the main path of contamination.

The study area investigated in Paper II and III is located in the Ronneby Municipality (Blekinge County) in Sweden. The landscape of the area is mainly represented by hilly terrain with woods surrounding urbanised areas. There are two main objects of interest considered. These include the F17 airfield (Blekinge Air Force Wing) and Brantafors Waterworks (Ronneby Municipality). The F17 (active since 1944) has been used by both military and civil air traffic. The airfield area is restricted and surrounded by wood in the north and west, and lake Sänksjön in the north. The F17 hosts both a flight exercise area and an operational wing (F17, 2020). The Brantafors waterworks has been in operation since the 1970s and at later development stages it supplied the Ronneby Municipality with drinking water. At Brantafors, source water for municipal water supply was extracted from the groundwater reservoir at four main extraction locations: north (GW1), south (GW3 and GW4), and east (GW2) (Paper III, Figure S1 in supplementary materials). The waterworks has been reconstructed and modified during its operation. There is, however, limited information available for the period prior to the 1990s. Prior to 2010, due to superior water quality (according to former standards), the water treatment process included aeration, pH adjustment, and UV-disinfection. Brantafors was later reconstructed, and the treatment was extended with aeration, chemical precipitation, rapid sand filtration, and UV-disinfection.

There are several surface water bodies in the studied catchment, including the Hasselstadsbäcken creek, the Klintabäcken creek, the Ronnebyån River, and the Lake Sänksjön (Paper III, Figure S1 in supplementary materials). Hasselstadsbäcken originates in the wetland area south-west of the Sänksjön and eventually discharges into Ronnebyån. Klintabäcken originates from the wetland areas in north and east of Sänksjön and discharges into Ronnebyån. Ronnebyån flows in a south direction and discharges into the Ronnebyfjärden Bay of the Baltic Sea. Lake Sänksjön is confined and primarily fed by groundwater and surface runoff (Paper III, Figure S1 and S4 in supplementary materials).

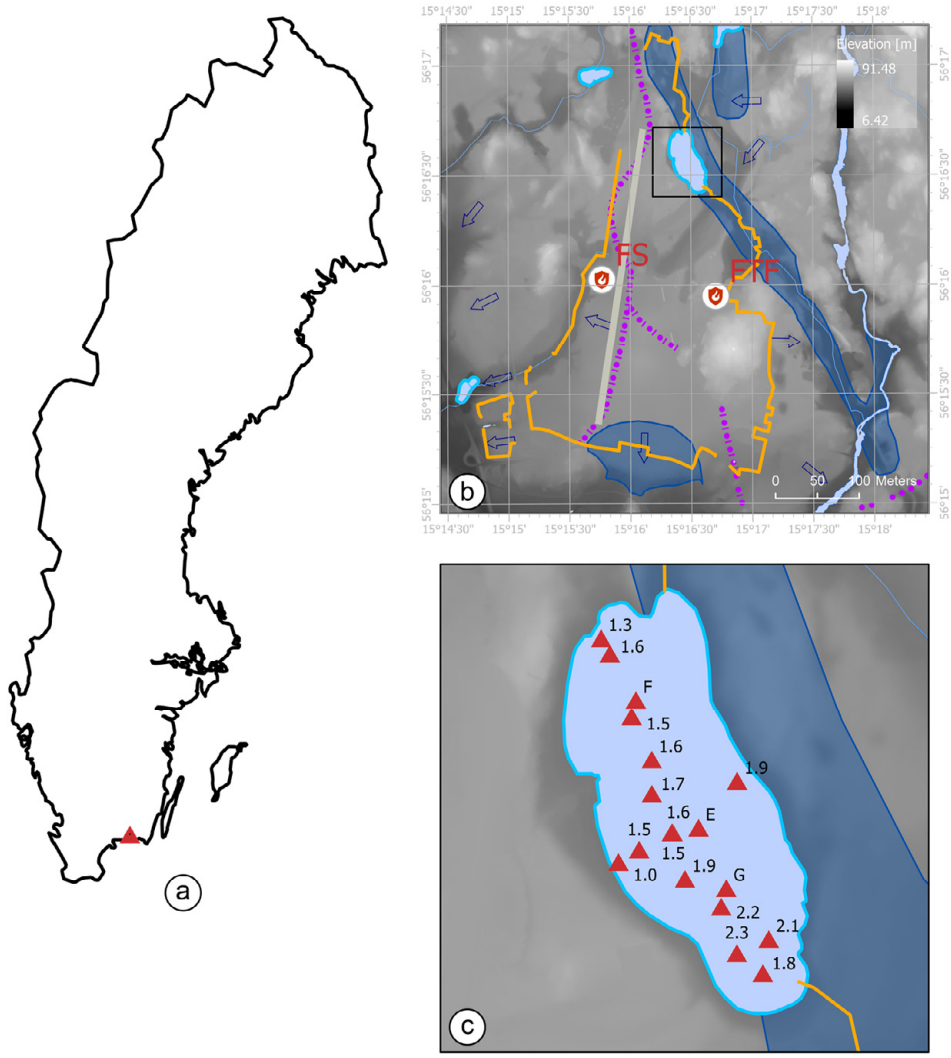

Figure 4. Study site description: (a) site location; (b) area topography and hydrogeology (including groundwater flow boundaries (purple dot-dash), flow direction (blue arrows) and reservoir (blue area)), airfield territory (solid orange), AFFF emission sources (fire station (FS) and fire training facility (FTF)) and lake location (black box); and (c) lake bathymetry and sampling locations. GIS data: GSD Terrängkartan vektor, Lantmäteriet (base map); GSD Höjddata, Lantmäteriet (topography) and SGU Grundvattenmagasin and Grundvatten, SGU (hydrogeology) (Figure 1 in Paper II).

The study area contains a groundwater reservoir confined by the groundwater divide along the airfield to the west and ridge formation along the Ronnebyån to the east

(Paper III, Figure S4 in supplementary materials). The groundwater reservoir is formed within a glacial deposit mainly containing a mixture of sand, silt, and gravel. The primary groundwater flow direction is southeast in a high-permeability soil formation along the Klintabäcken (Paper III, Figure S4 in supplementary materials). The groundwater reservoir is confined by the bedrock to the east and an upland with a thin soil layer (sand and silt), and shallow bedrock to the west. The bedrock morphology is primarily represented by granite, syenitoid, and metamorphic equivalents. The bedrock surface is characterised by deep and long fractures in direction from north to south (Paper III, Figure S5 in supplementary materials).

The studied Lake Sänksjön (S) (Paper II) is located approximately 100 m northeast of the F17 airfield. S has been contaminated by release of PFAS-containing AFFF at the airfield territory. There were two main emission sources suggested by Ronneby Municipality: fire training facility 900 m south and fire station 1200 m southwest of Lake S (Figure 4). Due to complex topographic and hydrogeological features of the area, it is difficult to conclude an exact PFAS emission source for the lake. According to the Swedish Geological Survey, the lake body confines an apparent connection to the underlying groundwater (Figure 4). However, despite PFAS contamination, the interaction with contaminated groundwater is unlikely due to groundwater flow direction and lake depth. Therefore, the PFAS transport to Lake S is suggested to be associated with surface runoff.

The overall PFAS emission in the area was primarily subject to application of PFAS-AFFF during fire-training activities and firefighting equipment tests at F17. The emission sources were connected to the designated fire-training and equipment test sites on the F17 airfield territory. Main emission source was identified at the fire-training facility (FTF), located in the east of the F17 airfield. However, there are several potential sources (training and test locations) suggested by former F17 personnel, including the north-end and south-end of the airstrip and the fire station (Paper III, Figure S1 in supplementary materials).

Sampling

In Luleå (Paper I), sampling was conducted on October 13, 2015. Duplicate surface water samples were collected at lake L (pH 7.7) and pond P (pH 7.9) using pre-rinsed 1 L polypropylene (PP) bottles. Water samples were stored at 8ºC prior to analysis. Sediment cores were taken in lake L from the bottom sediment at 7 m (location L1, 65°32'7"N, 22°5'57"E) and 19 m depth (location L2, 65°32'16"N, 22°5'41"E) (Figure 3). The sediment cores were collected using a manual sampler with transparent acrylic tube (50 cm long and 7 cm inner diameter) and piston-based mechanism. Sediment cores were sectioned by 1 or 2 cm intervals using a transparent acrylic slicer and distributed into pre-rinsed PP jars (n = 10 for core L1 and n = 13 for core L2). Sediment samples were kept frozen at –20ºC prior to analysis.

In Ronneby (Paper II), bathymetric measurements were conducted at Lake S using GPS receiver coupled with acoustic sonar on 16 June, 2017; measurements were taken at 18 locations with average water depth of 1.7 ± 0.34 m (Figure 4).

Duplicate water samples (bulk water) were collected at locations F and G (corresponding to north and south of the lake, respectively) at 1.6 m (F, $n = 2$) and 2.2 m (G, $n = 2$) water depth using 1 L polypropylene bottles and manual grab sampler on 20–21 June, 2016 (Figure 4).

Sediment core samples were collected at locations E–G (corresponding to centre, north and south of the lake, respectively) at 1.6 m (E), 1.6 m (F) and 2.2 m (G) depth on June 20–21, 2016. Sediment cores were extracted from the lakebed (in acrylic tube) using manual core sampler. Sediment cores E–G (with 0.34, 0.42 and 0.39 m of depth, respectively), were distributed in segments of 2 cm ($n = 17$, core E) and 3 cm ($n = 14$, core F; $n = 13$, core G).

All samples were stored at 3°C (water) and −20°C (sediment) prior to extraction and analysis. All sampling containers (polypropylene bottles, jars, acrylic slicer, and core tubes) were pre-rinsed with methanol (×5). Sediment sampler components (slicer and core tubes) were rinsed on site with Milli-Q water (×5) and methanol (×15) prior to each core sampling.

PFAS concentrations in groundwater were measured in samples collected at the extraction points GW1, GW3, and G4 in Ronneby (Paper III). Duplicate water samples were taken directly in the well (from the water surface) in 1 L PP bottles. Samples were stored in dark at 4°C. Prior to analysis, water samples (in 1 L PP bottle) were placed in sonication bath for 20 min. Samples were consequently transferred into 10 mL glass injection vial and spiked with internal standard mix prior to analysis.

Additionally, PFAS measurements in groundwater were taken using Polar Organic Chemical Integrative Sampler (POCIS) with solid phase sorbent (Oasis HLB). The individual POCIS sampler preparation was performed as described in Gobelius et al. (2019). Individual samplers (without cage) were set in a column configuration (Paper III, Figure S6 in supplementary materials) and placed in the groundwater well. There were two sampler columns deployed with eight individual samplers (4 duplicates) and three individual samplers (1 triplicate), respectively. Sampler columns were deployed in groundwater extraction wells upstream (POCIS x 8) and downstream (POCIS x 3) the groundwater aquifer at approximately 15- and 20-meter depth at extraction point GW1 and GW3, respectively (Paper III, Figure S4 in supplementary materials). For the well at GW3, a single deployment was set for 4 weeks, and at well GW1, four deployments were set for 1-to-4-week intervals. Individual samples were stored frozen prior to extraction and analysis.

Analysis and Measurements

PFAS analysis

As described in the enclosed papers (Paper I, II, III, and IV), up to 29 target compounds were analysed, including five perfluoroalkane sulfonates ($C_{4, 6, 7, 8, 10}$ PFSAs) (PFBS, PFHxS, PFHpS, PFOS, PFDS), 13 perfluoroalkyl carboxylates ($C_{3-13, 15, 17}$ PFCAs) (PFBA, PFPeA, PFHxA, PFHpA, PFOA, PFNA, PFDA, PFUnDA, PFDoDA, PFTriDA, PFTeDA, PFHxDA, PFOcDA), three perfluorooctane sulfonamides (FOSAs) (FOSA, MeFOSA EtFOSA), two perfluorooctane sulfonamidoethanols (FOSEs) (MeFOSE, EtFOSE), three perfluorooctane sulfonamidoacetic acids (FOSAAs) (FOSAA, MeFOSAA, EtFOSAA), and three fluorotelomer sulfonates FTSAs (6:2 FTSA, 8:2 FTSA, 10:2 FTSA). Furthermore, a mix of 16 mass labelled internal standards (i.e., $^{13}C_8$-FOSA, d_3-MeFOSAA, d_5-EtFOSAA, d_3-MeFOSA, d_5-EtFOSA, d_7-MeFOSE, d_9-EtFOSE, $^{13}C_4$-PFBA, $^{13}C_2$-PFHxA, $^{13}C_4$-PFOA, $^{13}C_5$-PFNA, $^{13}C_2$-PFDA, $^{13}C_2$-PFUnDA, $^{13}C_2$-PFDoDA, $^{18}O_2$-PFHxS, $^{13}C_4$-PFOS), and one injection standard (13C8-PFOA) were used for quantification.

The water sample extraction (Papers I and II) was conducted using the solid phase extraction (SPE) method (Powley et al., 2005; Ahrens et al., 2009). The extraction cartridge (Oasis WAX cartridges, Waters Corporation, MA USA) was preconditioned with mixture of ammonium hydroxide in methanol, methanol, and ultrapure water prior to extraction. Individual water sample was filtered (using glass fibre filter), spiked with an internal standards mixture, and loaded on the extraction cartridge with 1 drop per second. Subsequently, the extraction cartridge was washed with an ammonium acetate buffer in ultrapure water. PFAS were eluted with methanol and ammonium hydroxide solution in methanol. Samples were further concentrated under nitrogen and transferred to the auto-injector vial. The same extraction procedure was applied for all procedural blanks. All prepared samples were stored at -20°C prior to further analysis.

The extraction of the sediment samples (Papers I and II) was conducted using the solid-liquid extraction method (Powley et al., 2005; Taniyasu et al., 2005; Ahrens et al., 2009). The freeze-dried sediment samples were soaked in sodium hydroxide solution in ultrapure water and methanol. Further, samples were spiked with an internal standard mixture and extracted with methanol using wrist-action shaker. Subsequently, samples were centrifuged, supernatant was decanted and transferred, and the extraction process was further repeated; both extracts were combined, acidulated with hydrochloric acid, and centrifuged. The supernatant was transferred and concentrated under nitrogen gas. Concentrated samples were further mixed with ENVI-carb and glacial acetic acid in an Eppendorf tube using a vortex mixer and centrifuged; supernatant was further transferred into an auto-injector vial. The same

extraction procedure was applied for all procedural blanks. All samples were stored at -20°C prior to further analysis.

Extraction and preparation of the POCIS were performed in according to the method described earlier in Gobelius et al. (2019). There were 13 samples (including 2 procedural blank) extracted for analysis.

PFAS analysis was conducted in prepared samples (including procedural blanks) using high-performance liquid chromatography – tandem mass spectrometry (HPLC-MS/MS) (Papers I and II) and online SPE and ultra-performance liquid chromatography – tandem mass spectrometry (UPLC-MS/MS) (Papers III and IV). Limits of quantification were determined from levels detected in the procedural blank samples plus 3x of the standard deviation; or alternatively, at the lowest calibration point in the linear range (from 0.1 ng L^{-1} to 2000 ng L^{-1}) if the S/N ratio was higher than 3. Branched PFAS isomers were quantified with the analytical standard used for corresponding linear isomer.

Radio-isotope analysis

The analysis was performed on the corresponding replicate sediment samples (Papers I and II). Sediment accumulation rates were estimated from the detected excess 210Pb activity (disintegrations per minute per mass) in sediment samples. Sediment samples were homogenized and dehydrated (freeze-dried or dried in furnace at 50°C) prior to analysis. The constant rate of supply (CRS) model was used for age prediction. CRS model sediment accumulation rate estimate was compared against the linear regression estimate.

X-ray fluorescence analysis

Sediment elemental analysis was performed on the corresponding replicate sediment samples (Paper II) using the X-ray fluorescence (XRF) analyser in the soil mode. Samples were prepared and analysed in compliance with the US EPA method 6200 (EPA, 2007).

Dehydrated (freeze-dried) sediment samples were homogenized, weighed, and distributed into XRF sample cups and compressed between Prolene film (Chemplex Industries inc., Palm City, FL, USA) and glass fibre filter (Advantec, Tokyo, Japan). Polyester fibre wool was used as a dumper material. Individual samples were scanned two times (with X-ray beam collimated at the centre of the sample, and deviating from the centre) to improve the volumetric representation. Negative blank and positive reference samples (reference material NIST2709a, certified by Rigaku, Tokyo, Japan) were applied (every fifth sample and each core sequence) and analysed as an actual sample. Measured sediment sample concentrations were accordingly adjusted to the averaged negative blank levels.

Organic carbon, moisture content and density measurements

The sediment organic carbon and moisture content (Papers I and II) were determined on the replicate sediment core samples by combustion method (disaggregated samples were dried at 105°C and burned at 1350°C in a furnace).

Sediment bulk and dry bulk densities were determined from direct gravimetric and volumetric measurements on the wet and dehydrated sediment samples (Papers I and II).

Distribution predictors

The sediment-water partitioning coefficients K_d [L kg^{-1}] were calculated from the measured PFAS concentrations in sediment [µg kg^{-1}] and dissolved phase concentrations [ng L^{-1}] (surface water) (Paper I and II). The partitioning coefficients (K_d) were further normalized to the organic carbon content (f_{OC}) and expressed as carbon normalized sediment-water partitioning coefficient K_{OC} [L kg^{-1}] (EPA, 1999; Ahrens et al., 2010).

Sediment core analysis

Core analysis was implemented to investigate the PFAS composition and distribution in sediments. Estimated sediment accumulation rates (based on radio-isotope analysis) and measured PFAS concentrations were used to estimate the contaminant accumulation rates and indicate the contamination period (Paper I). Furthermore, PFAS distribution in sediment column was correlated with sediment organic and mineral contents, as well as sediment densities and moisture content (Paper II).

PFAS-AFFF emission estimates

The contaminant emission estimates were conducted using Monte Carlo simulations and accessible historical data (Paper III).

There is limited historical information available on AFFF use at the study site, as well as AFFF type or/and composition utilized in the past. The contaminant release was assessed in connection to suggested fire-training activities, equipment utilization, and AFFF release scenarios. PFAS was considered as an active AFFF surfactant and PFAS content in AFFF was estimated based on reported AFFF

compositions (Rupert et al., 2005). The surfactant (PFAS) and water release per individual training session (fire-training and and/or equipment test activity) was estimated according to the suggested equipment specifications and AFFF utilization scenarios. The annual emission scenarios were estimated as a cumulative release of individual training session scenarios per simulated period. An individual annual emission scenario was estimated from subsampled individual release scenarios considering possible variation of the training sessions per day (k), number of exercises per period (j), and number of events per year (i):

$$PFAS_{annual} = \sum_1^i \sum_1^j \sum_2^k m_{\,per\ session} \qquad \text{Eqn. (1)}$$

Data evaluation, calculations, and analyses were performed using Microsoft Excel (Microsoft, proprietary), Argo (Booz Allen Argo, open source), and MATLAB (MathWorks, proprietary) software. There is limited information available on exact PFAS composition in related PFAS-AFFF formulations (Place and Field, 2012; KEMI, 2015; Kärrman et al., 2016). Although, approximation on possible PFAS composition was possible, due to the historical nature of the contamination and possible variation in AFFF types, the PFAS emission estimates were restricted to "blind" PFAS. Thus, simulation estimates are subject to uncertainty.

Experimental setup

In Paper IV, the short-wavelength ultraviolet (UVC/VUV) induced treatment of PFAS was studied using an experimental setup. The setup was designed with emphasis on in-line treatment trails and used for analysis of the removal efficiency with perfluoro-sulfonamides (FASAs), fluorotelomer sulfonates (n:2 FTSAs), perfluoroalkyl carboxylates (PFCAs), and perfluoroalkane sulfonates (PFSAs).

Setup design

A laboratory scale UVC/VUV-treatment unit was set in a column configuration. Reaction chambers (columns x3) were consequently connected and looped to approximate an in-line treatment process. The irradiation source (UV lamp) was installed into the reaction chamber (column) using the immersion sleeve positioned in the centre of the column body. The system transport was controlled using the tubing looped at the sampling tank and peristaltic pump as a driver (Figure 5). Necessary material considerations were made for the reaction vessel and transport components to secure PFAS redistribution and sorption on the reaction chamber and transport channel surfaces. Furthermore, the reaction chamber dimensions were selected in order to optimise the exposure conditions (UV penetration and distribution in water).

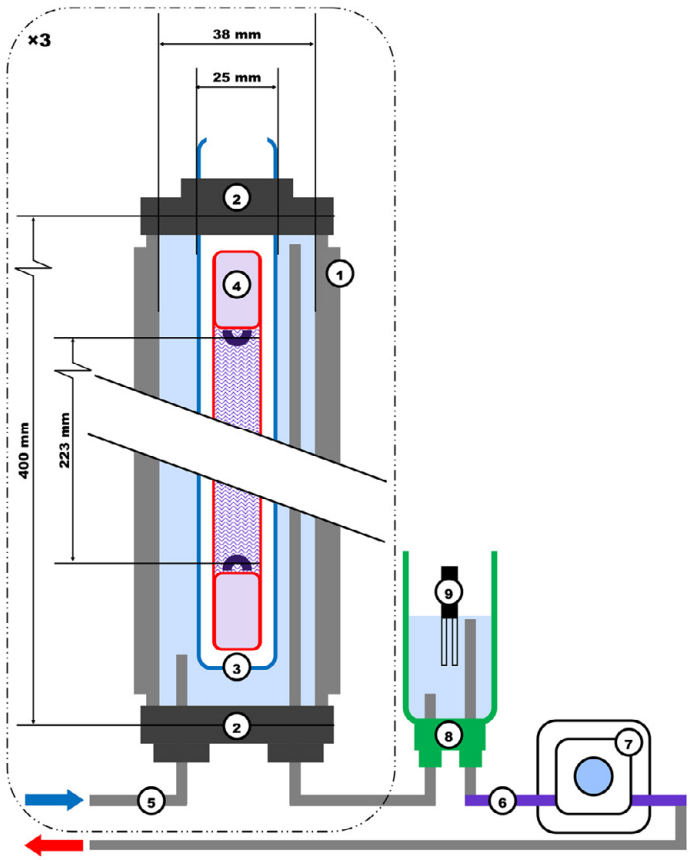

Figure 5. UVC/VUV treatment unit, dimensions, and description: 1) reaction chamber, 2) distributor and sleeve fitting, 3) immersion sleeve, 4) UV source, 5) transport tubing, 6) pump tubing, 7) peristaltic pump, 8) distributor and sampling chamber, and 9) auxiliary sensors (Figure 1 in Paper IV).

Experimental trials and quality control

In the experimental study (Paper IV), seven experimental trials were conducted. These, including trials with negative blank samples, perfluoro-sulfonamides and fluorotelomer sulfonates (positive blank and treatment samples), perfluoroalkyl carboxylates and perfluoroalkyl sulfonates (positive blank and treatment samples).

Treatment trials and sampling were conducted at different exposure conditions (15 to 600 min), system volume (0.8 and 1.1 L) and hydraulic residence time (6.6 to 13.2 min) settings (Table 7).

Samples were collected in duplicates, using polypropylene pipette tips (discarded after each duplicate sample); individual samples were transferred into pre-cleaned

(sonication in methanol x2) injection vials and spiked with an internal standard mix (20 µL). All samples were stored in dark at 4°C prior to analysis.

Prior to each experimental trial, the experimental setup was rinsed three times (methanol x1 and Milli-Q water x2), refilled, and set running (with no exposure) for an equilibration period of 10 hrs prior to measurements. Procedural positive samples were therefore corresponding to the equilibrated system base line concentrations.

Auxiliary measurements, including the solution pH, temperature, and conductivity were taken throughout the trials with the sensor installed in the sampling container.

Results and Discussion

Surface water

PFAS contamination was investigated in two lakes: L (including pond P) and S (Papers I and II). Both L and S, are located in a proximity to the airfields located in Luleå (F21) and Ronneby (F17), respectively. Water contamination in both lakes is connected to the application of PFAS-AFFF.

In Lake L (and adjacent pond P), 9 of the 26 investigated PFAS (i.e., PFBA, PFPeA, PFHxA, PFHpA, PFOA, PFBS, PFOS, PFHxS and 6:2 FTSA) were detected (Table 1). For both lake L and pond P water, the PFAS composition profile was dominated by PFSAs (70% of the ∑PFAS), followed by PFCAs (29%), whereas the contribution of 6:2 FTSA was low (<1%). For the PFSAs, PFHxS was dominant (48% of the ∑PFSAs), followed by PFOS (35%) and PFBS (17%). For the PFCAs, PFHxA was dominant (56%) of the ∑PFCAs, followed by PFPeA (14%), PFOA (12%), PFBA (11%), and PFHpA (7%).

Table 1. PFAS concentrations in duplicate water samples from the Lake L and pond P [ng L^{-1}] (Table 1 in Paper I).

	PFBA	PFPeA	PFHxA	PFHpA	PFOA	PFBS	PFHxS	PFOS	6:2 FTSA	ΣPFASs
L	53	72	280	34	58	200	570	410	8	1700
P	56	66	260	30	51	150	500	260	1.5	1400

In Lake S (measured at locations F and G), 8 of 26 investigated PFAS were detected (i.e., PFHxA, PFHpA, PFOA, PFNA, PFBS, PFHxS, PFOS, and 6:2 FTSA) (Table 2).

Table 2. PFAS concentrations in duplicate water samples from the Lake S measured at locations F and G [ng L^{-1}] (based on tables S4 and S5 in Paper II).

	PFHxA	PFHpA	PFOA	PFNA	PFBS	PFHxS-L	PFHxS-B	PFOS-L	PFOS-B	6:2 FTSA	∑PFAS
F	4.8	0.7	2.2	0.15	2.7	45	7.8	13	17	1.6	95
G	4.9	0.71	2.3	0.19	2.5	45	7.5	13	17	8.6	100

The ΣPFAS levels were identical at F and G (95 and 100 ng L^{-1}, respectively) and dominated by PFSAs, with a contribution of 84–90% for the sum of PFHxS and PFOS (including both linear and branched forms) to the overall PFAS content.

Contamination of the Lake L and Pond P (Paper I) is suggested to be connected to the PFAS emission from the same source (firefighting training facility at F21). This is due to identical PFAS concentration and composition detected in water samples. PFAS concentrations measured in water samples from L and P (ΣPFAS) were generally higher than in samples from other sites in Sweden (i.e., <80 ng L^{-1} ΣPFAS (Filipovic et al., 2015b) and <350 ng L^{-1} ΣPFAS (Ahrens et al., 2015); comparison was primarily restricted to the sites affected by PFAS-AFFF. High concentrations can be due to the longer water retention time in isolated water bodies (i.e., lakes, ponds) (Ahrens et al., 2015) as compared to runoff, rivers, and streams (Filipovic et al., 2015a; Filipovic et al., 2015b; Cousins et al., 2016). Thus, it is suggested that when interpreting detected PFAS levels, it is important to carefully consider water exchange and transport conditions. Furthermore, when PFAS contamination is primarily subject to AFFF application, the release scenarios, could play a role in interpretation of the detected levels (Cousins et al., 2016). Measured PFAS levels can be corresponding to an emergency PFAS-AFFF release (as in, e.g., Schiphol Amsterdam Airport, Netherlands, and L.B. Pearson Airport, Canada (Moody et al., 2002; Kwadijk et al., 2014)) or a historical emission (e.g., Flesland Airport in Norway (Kärrman et al., 2011)).

In the Lake S (Paper II), presence of PFAS can also be connected to PFAS-AFFF emission from the firefighting training facility at F17. Considering the lake volume (approximately 12×10^4 m^3), the total mass of PFAS in the water phase was estimated at approximately 12 g absolute. PFAS levels in water samples were in the same range as in measured surface water across Sweden (Gobelius et al., 2018). PFAS composition (predominated by PFHxS and PFOS) was identical to reported water samples from F18 airfield in Tullinge (suburb of Stockholm, Sweden) (Filipovic et al., 2015b), Arlanda Stockholm Airport, Sweden (Ahrens et al., 2015), and Schiphol Amsterdam Airport, Netherlands (Kwadijk et al., 2014).

Groundwater

In the analysed groundwater samples (Paper III) (corresponding to GW1, GW3, and GW4), there were 12 out of 29 analysed PFAS (PFBS, PFHxS, PFOS, PFDS, PFHpA, PFHxA, PFOA, PFNA, PFOcDA, 6:2 FTSA, 8:2 FTSA, and FOSA) detected (Table 3). PFAS analysis indicated high groundwater contamination levels at GW1 and GW3 with ∑PFAS concentrations of 4200±40 ng L^{-1} and 20000±1900 ng L^{-1}, respectively, followed by relatively low levels at GW4 with ∑PFAS of 18±3 ng L^{-1}.

In the groundwater corresponding to GW4, PFAS composition was primarily represented by PFOS (35%), PFHxS (32%), and FOSA (33%). At GW3, PFAS composition was dominated by PFOS (48%) and PFHxS (33%); followed by PFHxA (7%), PFOA (6%), PFBS (5%), and remaining compounds. Similarly, PFAS composition at GW1 was primarily represented by PFOS (72%) and PFHxS (19%), followed by remaining substances (<9%).

Table 3. Individual PFAS concentrations detected in groundwater samples from extraction points GW1, GW3, and GW4 [ng L^{-1}] (Paper III, table S1 in supplementary materials).

	PFBS	PFHxS	PFOS	PFDS	PFHpA	PFHxA	PFOA	PFNA	PFOcDA	6:2 FTSA	8:2 FTSA	FOSA
	<1	5.1	5.3	<5	<5	<10	<5	<5	<10	<10	<1	5.3
GW4	<1	5.4	6	<5	<5	<10	<5	<5	<10	<10	<1	5.4
	<1	5.2	5.8	<5	<5	<10	<5	<5	<10	<10	<1	5.5
	190	1400	2000	<5	86	280	260	<5	<10	<10	<1	5.7
GW3	200	1400	2000	<5	82	290	260	<5	<10	<10	<1	5.7
	180	1400	2100	<5	82	280	250	<5	<10	<10	<1	6.7
	340	3600	14000	<5	140	640	350	<5	<10	36	6.1	80
GW1	390	4300	16000	<5	150	720	390	8.8	12	41	5.5	93
	390	3700	13000	9.7	130	690	340	<5	46	36	5.9	82

PFAS concentrations measured at GW1 (north) and GW3 (south) are indicative in relation to the concentration gradient. PFAS concentrations are suggested to indicate a unified emission source affecting the groundwater from the north. Difference in the relative compositions is suggested to be connected to the contaminant mobility. For PFCAs (PFHxA-PFHpA-PFOA), the observed composition shifted from 58-12-30% at GW1 to 46-13-41% at GW3 (downstream). Whereas, composition of PFSAs (PFBS-PFHxS-PFOS) changed from 2-21-77% at GW1 to 5-39-56% at GW3. Furthermore, difference in detected levels (GW1 vs. GW3) for PFDA, PFNA, 6:2 FTSA, 8:2 FTSA, and FOSA is attributed to a possible effect of the molecular chain-length of the PFAS transport. However, PFAS distribution in the groundwater can be affected by different transport processes (including groundwater extraction and groundwater table variation) and sorption processes related to characteristics of the soil (Johnson et al., 2007; Hellsing et al., 2016; Weber et al., 2017). Therefore, until the contaminant transport conditions are sufficiently established, the suggested effect of the PFAS chain-length on transport should be considered with some precaution.

Analysis of the POCIS deployed in groundwater wells at GW1 and GW3 showed a slightly better method sensitivity (Paper III, Table S2 in supplementary materials). For PFCAs, detected in the samples corresponding to both GW1 and GW3, observed

PFAS composition was extended to PFPeA, PFHxA, PFHpA, PFOA, PFNA, and PFDA. It was also possible to conduct a semi-quantitative analysis of some branched PFAS, thus extending the inventory to L-PFHxS, B-PFHxS, L-PFOS, B-PFOS, L-FOSA, and B-FOSA (Figure 6).

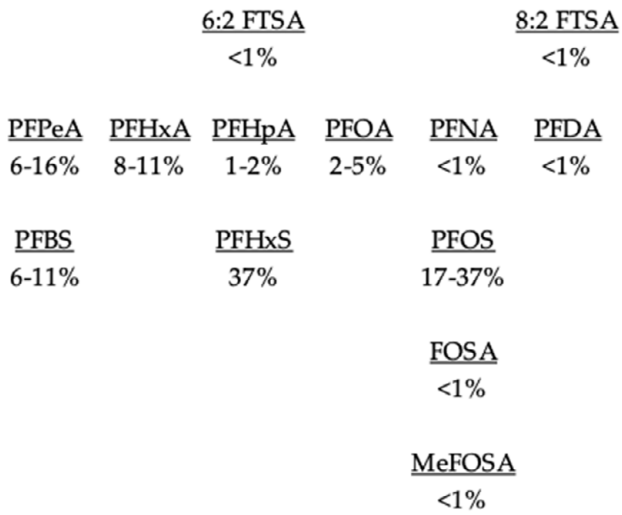

Figure 6. PFAS profile ("fingerprint") based on detected in POCIS deployed at GW1 and GW3 (sorted left to right in according to fluorinated chain-length) (Figure 1 in Paper III).

However, since the onsite calibration of POCIS was not possible and PFAS concentrations were estimated using the previously reported sampling rates (Gobelius et al., 2019), the analysis results were mainly considered for qualitative assessment. PFAS composition detected in POCIS was identical to those measured in groundwater samples and primarily represented by PFSAs (81% (GW1) and 65% (GW3)) and PFCAs (18% (GW1) and 35% (GW3)).

Sediment

PFAS concentration in the sediment (µg kg^{-1} dw) was analysed in sediment cores samples collected from Lake L and S (Paper I and II). There were two sediment cores analysed for Lake L (cores L1 (10 cm, *n*=10) and L2 (26 cm, *n*=13)) and three for Lake S (cores E (34 cm, *n*=17), F (42 cm, *n*=14), and G (39, *n*=13)), respectively.

In the sediment samples from Lake L (Paper I), 6 out of 26 investigated PFAS were detected, including PFBA, PFPeA, PFHxA, PFHxS, PFBS, and PFOS (Figure 7).

∑PFAS concentrations ranged between <1.0 µg kg^{-1} and 76 µg kg^{-1} dw. PFOS (<0.5–64 and < 0.5–23 µg kg^{-1} dw) and PFHxS (<0.5–7.4 and < 0.5–13 µg kg^{-1}dw), were predominant in both sediment cores (L1 and L2, respectively) (Figure 7). The average contributions of PFOS and PFHxS were 71% and 23% of the overall PFAS content, while the contribution of remaining PFAS was <7%. PFAS composition profiles for cores L1 and L2 showed identical patterns with maximum PPFAS concentration at top sections (1–4 cm). The SPFAS concentration decreased gradually from 76 to <2.0 µg kg^{-1} dw (L1) and from 42 to <1.0 µg kg^{-1} dw (L2).

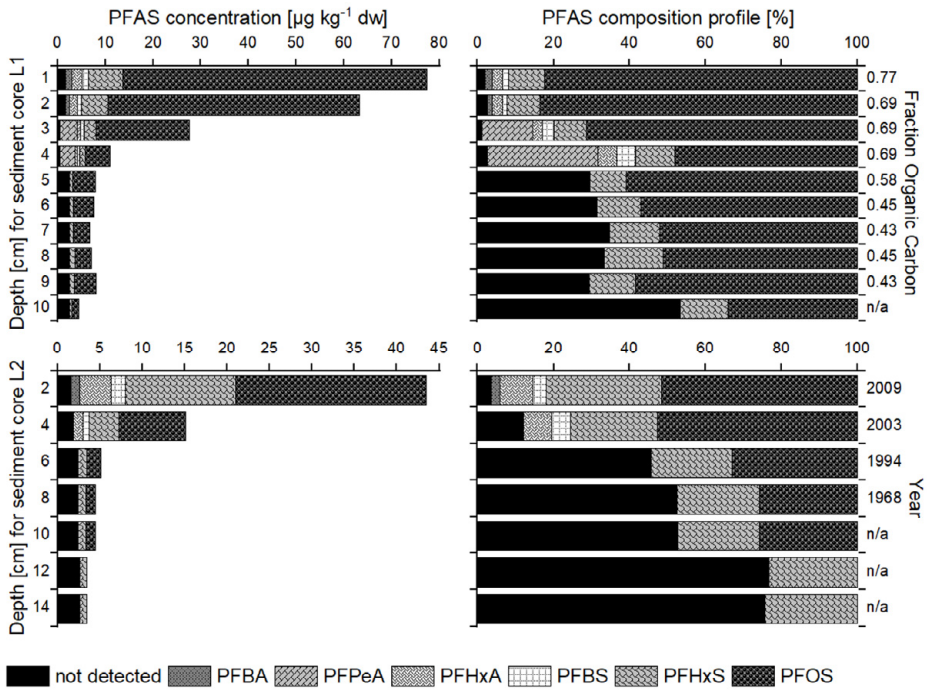

Figure 7. PFAS concentration [µg kg^{-1} dw] and relative composition by individual PFAS in sediment cores (L1 and L2) from lake L. The concentration and composition of the not detected PFAS were set to half of the respective detection limit; n/a = not available (Figure 2 in Paper I).

In studied sediments, maximum detected PFOS concentrations were 2–4 times higher than those reported for PFAS contaminated sediment samples [ng g^{-1} dw] from a creek at the L.B. Pearson Airport, Toronto, Canada (Awad et al., 2011) and channel at the Schiphol Amsterdam Airport, Netherlands (Kwadijk et al., 2014).

In the Lake S (Paper II), ΣPFAS concentration in sediment core samples ranged between 3.4–25, 4.9–38, and 3–61 µg kg^{-1} dw in core E, F, and G, respectively (Figure 8). PFAS composition in the sediment samples was identical and dominated

by PFSAs (PFHxS and PFOS as sum of linear and branched isomers) with the average contribution (n = 44) of 32 ± 11% for PFHxS and 22 ± 16% for PFOS, followed by 6:2 FTSA (21 ± 20%) and PFHxA (14 ± 9%).

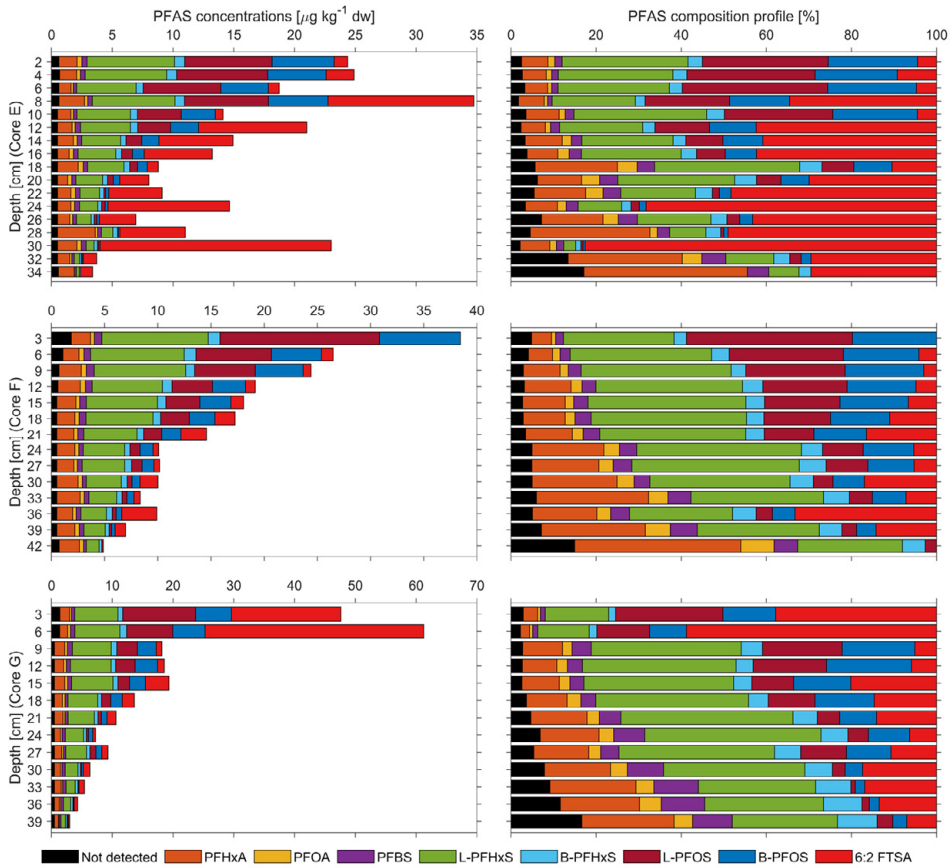

Figure 8. PFAS concentration [μg kg^{-1} dw] and relative composition by individual PFAS in sediment cores (E, F, and G) from Lake S; "not detected" includes concentrations of PFHpA, PFNA, PFDA, PFUnDA, PFDoDa, MeFOSAA, EtFOSAA and 0.5 MDL for the undetected PFAS (Figure 2 in Paper II).

For the remaining PFCAs (PFHpA, PFNA, PFDA, PFUnDA, and PFDoDa) and FOSAAs (MeFOSAA and EtFOSAA), the overall contribution was insignificant, as these compounds were inconsistently present in top sediment layers (0–12 cm) with total concentration of 0.6 (E), 2.4 (F), and 2.1 (G) μg kg^{-1} dw.

In sediment core from Lake S, vertical distribution of PFAS in the sediment column was considered as relatively even and dominated mainly by PFHxS and PFOS. However, the 6:2 FTSA concentration in sediment samples was elevated in the top

layer of Core G and ubiquitously present in sediment Core E (corresponding to south and centre of the lake, respectively). This, in agreement with elevated 6:2 FTSA concentration in the corresponding water samples (8.6 ng L^{-1} at location G) may indicate a recent emission or source located in the south of the lake.

Measured PFAS concentrations (dw) in sediments were similar to those reported for Schiphol Amsterdam Airport (Netherlands), whereas PFHxS concentrations were one order of magnitude higher (Kwadijk et al., 2014). The PFAS composition was similar to sediments from Lake Halmsjön (Sweden) (Ahrens et al., 2015). The elevated 6:2 FTSA levels were similar to sediment from Lake Langavatnet (Norway) (Kärrman et al., 2011). ∑PFAS concentrations in surface sediment (dw) were 1–10 times higher than reported for Laurentian Great Lakes (Canada-US) (Remucal, 2019).

Distribution predictors

Sediment-water partitioning coefficients K_d (L kg^{-1}) and sediment organic carbon normalised partitioning coefficients K_{OC} (L kg^{-1}) were estimated based in PFAS concentrations detected in lake water samples and sediment core samples (Paper I and II).

For Lake L (Paper I), sediment-water partitioning coefficients were derived from PFAS concentrations detected in bulk water samples (ng L^{-1}) and sediment samples (µg kg^{-1} dw) corresponding to the top layers in core (1–2 cm, L1) (Table 4).

Table 4. log K_d (sediment–water partitioning [L kg^{-1}]) coefficients and log K_{OC} (organic carbon normalised sediment–water partitioning [L kg^{-1}]) coefficients for sediment (1-2 cm surface layers) at Lake L (Table 1 in Paper I). *) note: a miscalculation was found in K_{OC} estimates, thus presented values correspond to corrected from these stated in the original table (Table 1 in Paper I).

	PFBA	PFHxA	PFBS	PFHxS	PFOS
Log Kd (L1)	1.4	0.9	0.8	1.1	2.19
Log Kd (L2)	1.2	0.8	0.6	1.0	2.1
*Log K_{OC} (L1)**	3.5	3.0	2.9	3.2	4.31
*Log K_{OC} (L2)**	3.4	2.9	2.8	3.15	4.27

Connection between perfluoroalkyl chain length (CF_2 moiety) and partitioning coefficients (K_d and K_{OC}) was relevant for PFSAs (Higgins and Luthy, 2006; Ahrens et al., 2009; Ahrens et al., 2011); whereas no trend was observed for PFCAs.

The sediment log K_{OC} values were in agreement with previous studies in freshwater systems (Kwadijk et al., 2014), whereas the sediment log K_{OC} was approximately one log unit lower than reported previously in saline water systems (Ahrens et al.,

2010; Ahrens et al., 2011). The partitioning of PFAS might have been impacted by the sediment mineral content (i.e., electrostatic surface interactions) (Johnson et al., 2007; Hellsing et al., 2016) or solute metal ion concentrations (Higgins and Luthy, 2006). Structural, solution-specific, and medium related parameters need to be considered to explain the partitioning behaviour of PFAS in solid-aqueous phase systems. For the estimation of sediment sorption coefficients, the concentration ratio for dissolved and sorbed phases is universally considered as a system at equilibrium (Baum, 1997). However, the assumption of equilibrium is not always applicable in natural systems, where a certain mass exchange normally exists between water bodies (Krabbenhoft et al., 1990; Sacks et al., 1998). In the given system, the PFAS equilibration process is strongly impacted by extensive seasonal spikes (during the spring) from the surface flow (runoff) (Bengtsson and Westerstrom, 1992). Furthermore, an exchange with groundwater might contribute to a continuous dilution of the contaminated lake water. Thus, despite agreement with previously reported values, the provided sediment-water partitioning coefficients should be considered with a certain precaution (Xiao, 2015).

For the distribution predictors investigated at Lake S (Paper II), K_d (L kg^{-1}) and K_{OC} (L kg^{-1}) coefficients were estimated based on PFAS concentrations in water samples (ng L^{-1}) collected close to the bed surface (F and G) and sediment core sample concentrations (µg kg^{-1} dw) throughout the entire core (F and G).

Table 5. Log K_d (sediment–water partitioning [L kg^{-1}]) coefficients and log K_{OC} (organic carbon normalised sediment–water partitioning [L kg^{-1}]) coefficients for sediment at Lake S (Table S9 in Paper II).

	PFHxA	PFOA	PFBS	L-PFHxS	B-PFHxS	L-PFOS	B-PFOS	6:2 FTSA
K_d (F)	2.3 ± 0.08 (14)	0.63 ± 0.06 (14)	1 ± 0.13 (14)	5.62 ± 0.29 (14)	2.48 ± 0.18 (14)	3.48 ± 0.61 (14)	3.92 ± 0.43 (13)	0.66 ± 0.26 (12)
K_{OC} (F)	4.33 ± 0.07 (14)	2.63 ± 0.06 (14)	3.02 ± 0.13 (14)	7.62 ± 0.27 (14)	4.49 ± 0.18 (14)	5.49 ± 0.62 (14)	5.94 ± 0.45 (13)	2.68 ± 0.24 (12)
K_d (G)	2.15 ± 0.12 (13)	0.57 ± 0.17 (13)	0.92 ± 0.12 (13)	5.48 ± 0.34 (13)	2.39 ± 0.17 (13)	3.23 ± 0.76 (13)	3.67 ± 0.66 (13)	3.02 ± 0.63 (13)
K_{OC} (G)	4.18 ± 0.11 (13)	2.6 ± 0.15 (13)	2.95 ± 0.1 (13)	7.53 ± 0.32 (13)	4.42 ± 0.16 (13)	5.27 ± 0.77 (13)	5.68 ± 0.65 (13)	5.05 ± 0.6 (13)

In core F and G, K_d and K_{OC} values were consistent for PFHxA, PFOA, PFBS, PFHxS, and PFOS, except for 6:2 FTSA. For PFSAs, there was an increase observed in K_d and K_{OC} values in connection to perfluorocarbon moiety as PFBS < B-PFHxS < L-PFOS ≈ B-PFOS, except for L-PFHxS. There was no relation with perfluorocarbon chain length observed for PFCAs (Table 5). The K_{OC} values were generally higher than K_d values, indicating an affinity of PFAS to organic carbon, which agrees with previous studies (Ahrens et al., 2011; Jeon et al., 2011; Remucal, 2019). However, it is suggested to consider the field derived K_{OC} values with a certain precaution. Due to the surfactant nature of PFAS and related interaction mechanisms with surfaces, the organic carbon normalized K_{OC} may not fully represent the medium (Xiao, 2015; McCarthy et al., 2017a).

Field-derived log K_d values were slightly higher than reported for corresponding PFAS in lake sediments at Stockholm Arlanda Airport (Ahrens et al., 2015) and river sediments at Schiphol Amsterdam Airport (Kwadijk et al., 2014). For PFOS, log K_d values were about two times larger than reported for marine sediments (Ahrens et al., 2011; Chen et al., 2012). It is important to note that PFAS concentrations in sediments can be a result of a recent release or historical emission (Awad et al., 2011; Zareitalabad et al., 2013; Filipovic et al., 2015b). Hence, unless the spatial and temporal conditions are established, field-derived K_d values should be considered with a certain precaution, as well as the local equilibrium conditions need to be properly established.

Core analysis

Primary objective of the core studies conducted at the Lake L was to evaluate contamination history of the PFAS exposed recipient (Lake) and estimate the PFAS accumulation rates (Paper I).

The radioisotope analysis was conducted on the replicate sediment samples corresponding to core L2. The sediment accumulation rates were estimated based excess radioisotope activity (^{210}Pb/^{226}Ra) measured in corresponding sediment core samples. The estimated uncertainty of the analysis was ±11% for the detection between 0.6 and 40 dpm g^{-1} (disintegrations per minute per mass) at 95% confidence interval.

The constant rate of supply (CRS) model was used for sediment age prediction (Sanchez-Cabeza et al., 2000; Swarzenski, 2013). The CRS average sediment accumulation rate estimate shows agreement with the linear regression estimate (at 0.4 kg m^{-2} yr^{-1}). Sediment accumulation rates (CRS model) calculated for core L2, showed a decrease with depth from 9.2 kg m^{-2} yr^{-1} (2–4 cm) and 8.4 kg m^{-2} yr^{-1} (4–6 cm) to 0.29–0.31 kg m^{-2} yr^{-1} (6–12 cm); at the surface layers the accumulation rate was estimated as 0.3 kg m^{-2} yr^{-1}. The decrease in sediment accumulation rate, as well as rapid increase in the sediment bulk density, beginning at 8 cm depth is suggested to represent the "younger" sediment (less than 50 years old) overlying an older base sediment (between 1968 and 2009); thus, reflecting the lake sediment formed (accumulated) on an artificially excavated reservoir.

The estimated PFAS accumulation rates showed an increased activity for the period post 2003 with a flux of 12 µg m^{-2} yr^{-1}1 dw for ΣPFAS. The PFAS flux increased from 2.3 mg µg m^{-2} yr^{-1}1 dw in 1994 to 11 µg m^{-2} yr^{-1}1 dw by 2009. Over the accumulation period between 1994 and 2009, the lake sediment surface (corresponding to L2) received ΣPFAS of 213 µg m^{-2} yr^{-1}1 dw (65 µg m^{-2} yr^{-1}1 dw for PFHxS and 125 µg m^{-2} yr^{-1}1 dw for PFOS). Based on observations, the PFAS accumulation is suggested to have started approximately in 1994 (Figure 9).

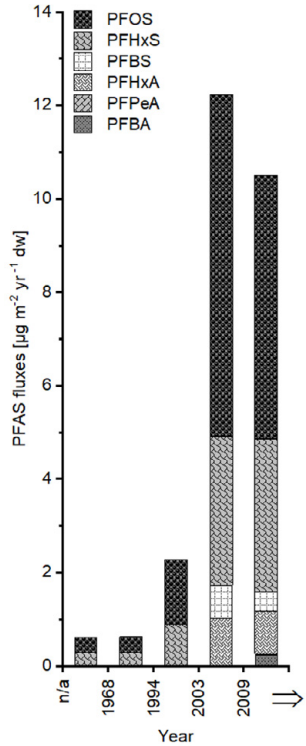

Figure 9. PFAS accumulation in the sediment (corresponding to L2) estimated for the suggested period (Figure 3 in Paper I); Note (not reflected in the enclosed study (Paper I)): it was later confirmed from other sources, that according to workers at the excavating company, the excavation below the groundwater surface (currently confining the Lake L) was active between 1974 and 1998 and completed in 2000. Thus, there was no lake in 1968; and thus, the estimated PFAS accumulation rates can only be valid for the period starting from 1994.

Furthermore, correlation between PFAS concentrations in sediment and sediment fraction organic carbon (f_{OC}) was tested. PFHxS ($r=0.73$, $p<0.026$) and PFOS ($r=0.74$, $p<0.023$) were found positively correlated (Pearson pairwise) with sediment f_{OC}.

Identically to core analysis described above (Paper I), the study of Lake S (Paper II) the initial objective of the analysis was to evaluate the contamination history of the PFAS exposed recipient (Lake S). This was done to obtain an indicator of the overall contamination period at the studied site.

There were two independent core investigations (radioisotope analysis vs. PFAS analysis) conducted in 2016 and 2017 (not included in the appended study (Paper II)). Unfortunately, assessment of the sediment accumulation rates and PFAS temporal distribution was not possible due to inconclusive analysis results. On the first core analysis attempt (10.5 cm deep core with 1.5 cm per section), the radioisotope analysis ($^{210}Pb/^{226}Ra$) on the replicate sediment core samples showed

inconsistency in estimated sediment accumulation rates (CRS). The sediment accumulation rates were deviating from 0.0041 kg m^{-2} yr^{-1} at the age at the bottom of extrapolated core section of <200 years (6–8 cm) to 0.0052 kg m^{-2} yr^{-1} at <160 years; and to 0.0036 kg m^{-2} yr^{-1} at <120 years (4–6 cm); and further 0.004 kg m^{-2} yr^{-1} at <60 years (2–4 cm) and to 0.0059 kg m^{-2} yr^{-1} at <40 years (0–2 cm). In the second attempt, cores were resampled at different location and core segmentation was changed to 3 cm per section. However, the radioisotope analysis (^{210}Pb) was not conclusive due to very weak signal from the sediment samples. The radiocarbon (^{14}C) analysis was considered as an alternative. However, application of the radiocarbon analysis was later dropped due to risk of interference from possible modern carbon deposits in the sediment.

The sediment core study for Lake S was further extended to investigation of the influence of sediment specific characteristics on PFAS distribution (Paper II). Therefore, an additional core analysis was performed with combination of PFAS analysis and XRF analysis.

The sediment core samples from the Lake S (Paper II) were identified as fine detritus gyttia (E) and coarse detritus gyttia (F and G). Sediment densities were consistent in sediment cores E, F, and G with the average density of 1.0 ± 0.06, 0.97 ± 0.05 and 0.98 ± 0.03 kg L^{-1}, respectively. The average fraction of organic carbon (f_{OC}) was 0.96 ± 0.03, 0.95 ± 0.04 and 0.95 ± 0.07 for sediment cores E, F, and G, respectively. The mean dry bulk density ($\rho_{dry\ bulk}$), however, was slightly lower in core F (0.03 ± 0.01 kg L^{-1}) than in cores E and G (0.04 ± 0.01 and 0.04 ± 0.02 kg L^{-1}, respectively). The sediment in cores (E, F, and G) were considered identical and mostly represented by organic matter (Paper II, Table S1 in supplementary materials).

Based on XRF analysis, the sediment mineral content in cores F and G was represented by sulphur (12.000 ± 2900 and 13.000 ± 1900 mg kg^{-1} dw, respectively), iron (9100 ± 1600 and 9100 ± 2300 mg kg^{-1} dw, respectively) and calcium (6800 ± 1500 and 14.000 ± 2800 mg kg^{-1} dw, respectively) (Paper II, Tables S10 and S11 in supplementary materials).

The relationship between individual PFAS concentrations and sediment fraction organic carbon, densities, and moisture content was studied for four PFCAs (PFHxA, PFHpA, PFOA and PFUnDA), three PFSAs (PFBS, L-PFHxS, B-PFHxS, L-PFOS and B-PFOS), MeFOSAA and 6:2 FTSA. Out of eleven studied PFAS, only long-chained PFUnDA ($r = -0.8$, $n = 8$) and L-PFOS ($r = -0.4$, $n = 43$) showed a negative correlation ($p < 0.05$) with fraction organic carbon (Paper II, Table S12 in supplementary materials). All PFSAs and PFOA showed a weak negative correlation with bulk sediment density. For the dry bulk density, PFHxA ($r = -0.4$, $n = 44$), PFOA ($r = -0.8$, $n = 43$) and PFBS ($r = -0.5$, $n = 44$) showed a negative correlation (Paper II, Table S12 in supplementary materials). There was no significant correlation with the moisture content observed.

Correlation between individual PFAS concentrations and sediment elemental content was studied for PFHxA, PFOA, PFBS, PFBS, L-PFHxS, B-PFHxS, L-PFOS, B-PFOS, and 6:2 FTSA (n = 26) (Paper II, Table S13 in supplementary materials). All PFSAs showed a positive correlation ($p < 0.05$) with sulphur (r_s = 0.5–0.6) and titanium (r_s = 0.5–0.6); moreover, for long-chained PFSAs (i.e., PFHxS and PFOS), a positive correlation was found for sediment lead (r_s = 0.6–0.7), arsenic (r_s = 0.6–0.7), and iron (r_s = 0.5–0.6). For PFCAs, PFHxA showed a positive correlation with sediment rubidium, (r_s = 0.4) lead (r_s = 0.6), and arsenic (r_s = 0.6) and a negative correlation with calcium (r_s = −0.5). PFOA was positively correlated with sediment lead (r_s = 0.5), arsenic (r_s = 0.4), and titanium (r_s = 0.4).

Principal component analysis (PCA) was performed on standardized parametric data (n = 26, sediment cores F and G) (Figure 10). The overall data variability was sufficiently explained as 43, 24, and 12% within the first three component spaces (Paper II, Figure S1 in supplementary materials). Within the first component space (43% variation explained), the long-chain PFSAs (L-PFHxS, B-PFHxS, L-PFOS, and B-PFOS) followed by sediment arsenic and lead had strong contribution to the data variability. For the short-chain PFBS, sediment rubidium and titanium contributions were identical on the lower level. L-PFOS, sediment iron and sulphur had a similar contribution to the variance within both first and second component spaces (<67% variance explained). PFCAs and contravariant dry bulk density contributions were relevant within first and (on greater level) second component spaces. Contribution of the fraction organic carbon and moisture content was relevant within the second component space only and represented by <24% data variability. Overall, PFSAs variation showed an alignment (correlation) with sediment arsenic, lead, rubidium, titanium, and sulphur. PFCAs were negatively correlated to dry bulk density. There was no clear correlation between individual PFAS and fraction organic carbon.

In the studied sediments, long-chain PFCAs and PFSAs showed significant correlation with sediment lead, arsenic, iron, titanium, and sulphur ($p < 0.05$). This is in agreement with previous studies, indicating a major effect of the electrostatic interaction with the mineral content of the medium (Jeon et al., 2011; Hellsing et al., 2016). The slightly stronger correlation with sediment dry bulk density (r_s = −0.6–0.7) may indicate the association with aqueous phase and the mechanical impact of media pore space on PFAS distribution.

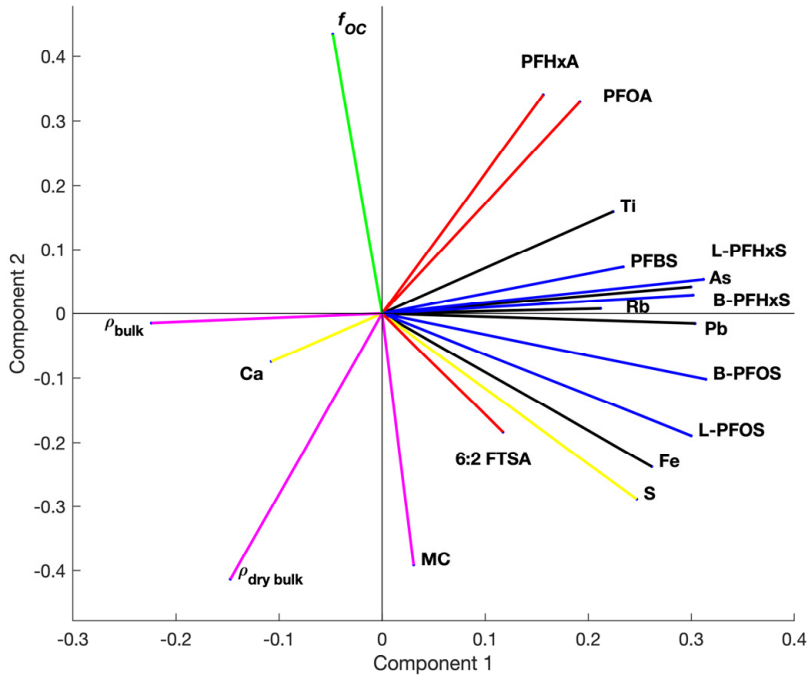

Figure 10. Bi-plot of parameter contribution of data variance within the first (43% explained) and second (24% explained) component spaces, including PFCAs and FTSA (red); PFSAs (blue); sediment iron, lead, rubidium, arsenic and titanium (black); sediment sulfur and calcium (yellow); sediment densities ($\rho_{dry\ bulk}$ and ρ_{bulk}) and moisture content (MC) (magenta); and fraction organic carbon (f_{OC}, green) (Figure 3 in Paper II).

Measured sediment elemental content was primarily subjected to the solid phase. This is due to lacking significant correlation with sediment dry bulk density and moisture content. However, inorganic content was measured in bulk dried samples and can represent both matter of the solids and corresponding species (or/and complexes) in aqueous phase (EPA, 1999). Previous studies have shown that sorption of PFAS is impacted by pH and suggested to decrease in K_d values with increasing pH, which is most likely due to pH depending changes in zeta potential of the solid surface (Higgins and Luthy, 2006; Johnson et al., 2007). It is suggested that the partitioning of PFAS (in particular long-chained PFSAs) in natural media could be affected by the presence of metal oxides and metal-ligand complexes (carbonate, sulphate or phosphate ligands) in aqueous phase. This was, however, beyond the scope of the study.

PFAS-AFFF profiling

Identification of possible PFAS-AFFF formulations was conducted based on cross-evaluation of the individual PFAS detected in POCIS (Paper III) and elsewhere reported PFAS compositions detected in PFAS-AFFF samples (Table 6).

There are a few possible PFAS-AFFF types suggested. The PFSAs based PFAS-AFFF (often referred as Legacy foam) is suggested to be the major contributor to PFAS emission. This is in connection to the PFSAs (PFBS, PFHxS, and PFOS) profiles observed in the groundwater samples. The PFCAs composition, on the other hand, is attributed to PFCAs/FTSAs based PFAS-AFFF and alternatively to FTSAs based PFAS-AFFF (assuming possible FTSAs to PFCAs transformation) (Kissa, 2001; Buck et al., 2011; KEMI, 2015).

Furthermore, traces of perfluoroalkane sulphonamides substances such as FOSA and MeFOSA, are considered as an indicator of the fluorination method used for production of the corresponding PFAS. FOSA and MeFOSA can be linked to the PFAS synthesis involving electrochemical fluorination (Buck et al., 2011). Thus, the detected FASAs are associated with the raw material used in electrochemical production of detected PFSAs (PFBS, PFHxS, and PFOS) and indirectly confirming the PFSAs based origin of PFAS-AFFF. The PFCAs (PFPeA, PFHxA, PFHpA, PFOA, PFNA, and PFDA) detected in the groundwater samples can be attributed to electrochemical fluorination as well as fluorotelomer processes (Buck et al., 2011). FTSAs, on the other hand, can strictly be associated with the fluorotelomer process-based origin. Assessment of the PFSAs vs. FPCAs and FTSAs traces, as well as analysis of the FASAs, are useful in identification of the synthesis processes and related PFAS-AFFF origin (Moody and Field, 2000; Kärrman et al., 2011; Kärrman et al., 2016).

However, PFAS-AFFF identification based on measured PFAS composition in groundwater is neglecting possible effects of transport and retention. Thus, detected PFAS composition may not fully represent the actual PFAS composition in PFAS-AFFF. The assumptions on the PFCAs/FTSAs based PFAS-AFFF should be considered with precaution. Further investigation is necessary to establish the transport conditions and confirm the connection between PFAS in groundwater and emission source.

Table 6. PFAS compositions detected in available PFAS-AFFF samples (based on table S3 in Paper III).*

(*) shown PFAS compositions nor concentrations might not fully represent the actual PFAS composition in PFAS-AFFF, (1) corresponding to US market, (2), corresponding to Swedish market, (3) used in 1980s–2008, (4) used in 1980s–present, (5) unspecified period of use by 2014, (6) individual PFAS with possibly different functional group configuration than stated (Place and Field, 2012; KEMI, 2015)

PFAS detected in sample	3M [1,3]	National Foam [1,4]	Ansul [1,4]	Angus [1,4]	Chemguard [1,4]	Fire Service Plus [1,4]	OneSeve B-AR [2,5]	ARC Miljö [2,5]	Towalex AFFF-AR 3x3 [2,5]	Towalex AFFF 3% Master [2,5]	Sthamex AFFF-P 3% [2,5]
PFBA	?						27%	10%	5%	7%	1%
PFPeA	?						20%	2%	3%	4%	
PFHxA	?						9%	18%	49%	62%	1%
PFHpA	?						2%		1%	1%	
PFOA	?								1%	2%	
PFDA	?								1%	1%	
PFBS	x%[6]										
PFHxS	x%										
PFHpS	x%										
PFOS	x%										
10:2 FTSA		x%[6]		x%[6]	x%[6]	x%[6]	?	?	?	?	?
8:2 FTSA		x%[6]	x%[6]	x%[6]	x%[6]	x%[6]	?	?	?	?	?
6:2 FTSA		x%[6]	x%[6]	x%[6]	x%[6]	x%[6]	43%	71%	41%	24%	98%
4:2 FTSA		x%[6]				x%[6]	?	?	?	?	?

AFFF emission estimates

Simulation of the potential PFAS release (production) scenarios was conducted for an individual fire-training session, as well for a possible annual emission.

The individual fire-training session scenarios were simulated considering possible variation in the AFFF stock solution composition, surfactant composition (PFAS content), AFFF solution, and equipment utilisation. For the AFFF stock solution composition, prior population boundaries were assigned as [0.5 <.065±0.21 <0.9] for water content, [0.1 <0.17±0.054 <0.24] for surfactant content (not restricted to PFAS), and [0.5-1] as an additional parameter for surfactant composition (or PFAS content) (Rupert et al., 2005; Place and Field, 2012). AFFF dilution scenarios were estimated based on reported and suggested by F17 former personnel (with prior population set as [0.01 <0.03 <0.04]). With suggested equipment utilization

scenarios, the PFAS emission per an individual training session [kg] was estimated as [1.4 <11.5±5.7 <43.7] (n=20000, average deviation (adev)=4.5). Similarly, release of water [L] corresponding to content in AFFF, was estimated as [945 <1985±594 <3032] (n=20000, adev=515). Furthermore, with suggested exercise routine, the annual PFAS emission rate [kg yr^{-1}] was estimated as [6 <414±436 <5462] (note: these values correspond to one individual simulation (n=20000)) (Figure 11).

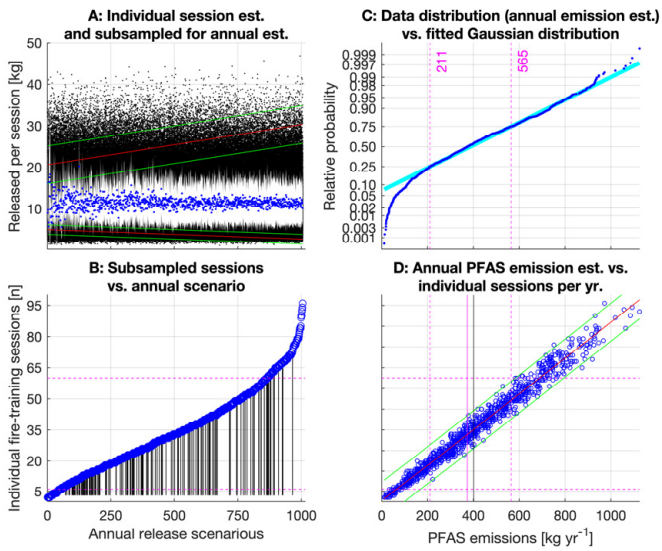

Figure 11. Evaluation the PFAS emission scenarios. A: black dots represent simulated individual PFAS emission scenarios (corresponding to an individual fire-training session); blue dots represent the mean of the subsampled n-scenarios with white area corresponding to ± one standard deviation; red line at top and bottom represent the maximum and minimum of the subsampled n-scenarios respectively, with green lines corresponding to ± one standard error. Vertical axe corresponds the variation in individual emission scenarios and horizontal axe corresponds to set of individual samples (n=20000 ×1005). B: blue circles indicate the number of subsampled session scenarios in A; vertical black lines correspond to suggested most-likely exercise routine with 3 consequent training days per annual exercise occurrence. C: comparison of the distribution of the simulated annual release scenarios (blue dots) vs Gaussian distribution (cyan); vertical dashed magenta lines correspond to first and third quantiles of the data. D: Estimates on annual PFAS emission (blue line) vs number of individual training sessions, shown as a linear fit with green line corresponding to ± three standard deviations; vertical magenta line corresponds to estimated median, vertical black line corresponds estimated mean, and dashed vertical magenta lines correspond to first and third quantiles of the data (Figure 2 in Paper III).

The annual release scenarios were evaluated based on subsamples from simulated individual emission scenarios (per fire-training session). Subsampling and calculations were conducted using suggested fire-training exercise routines (including 2-6 individual sessions per day, 1-5 training days, with 1-5 occurrences per year); there were 1005 annual release scenarios evaluated (Figure 11).

The estimated annual emission scenarios varied between [11 <401±233 <1125 kg yr^{-1}], corresponding to [2 <35±20 <96] individual fire-training sessions per year (n=1005) (Figure 3). With further approximation, the annual PFAS emission can be estimated for the suggested most-likely exercise routine scenario as 3 consequent training days per occurrence and 2–4 occurrences per year. Thus, for the scenario with 6–60 individual sessions carried out per year (with 1-5 sessions, 3 training days, and 1-4 occurrences per year), the annual emission range is approximately 100–700 kg per year. However, since the annual emission scenarios are based on a rather limited sample, given estimates are strictly relative to evaluated population. Further investigation is necessary to validate the estimate accuracy.

Due to limited data available for both possible PFAS-AFFF composition and historical records of AFFF use at the studied site, it was not possible to estimate the individual PFAS emission. The estimates of PFAS release were conducted with no restriction to actual PFAS composition in the PFAS-AFFF stock solution. The overall surfactant composition in the PFAS-AFFF was considered to include fluorinated (PFAS) and non-fluorinated surfactants. There is, however, limited information available regarding the surfactant composition as well as exact PFAS-AFFF formulation (type).

PFAS estimates were made in an attempt to reconstruct the historical emission as in connection to PFAS-AFFF release scenarios and fire-training activities. Calculations were made in a semi-quantitate manner, considering the range of both PFAS-AFFF contents and application scenarios. However, for an accurate assessment, it necessary to further clarify the AFFF application history. This including the PFAS-AFFF stock solution formulations, PFAS/surfactant composition in AFFF, and AFFF application routine (frequency and duration).

Transport considerations

In Paper III, PFAS emission was connected to the PFAS-AFFF application during fire training and equipment test at FTF. The spatial distribution of PFAS and contamination of the aquatic environment is primarily associated with transport in the dissolved state, including transport with surface runoff, advective-diffusive transport with groundwater, and further distribution with raw water extraction (Figure 12).

The initial stage of emission was associated with fire-training activities at FTF (Paper III, Figure S1 in supplementary materials). Training activities included simulation of the offsite aircraft rescue missions. Primary AFFF application was connected to dispatch of the rescue vehicle and putdown of an open fuel pool fire.

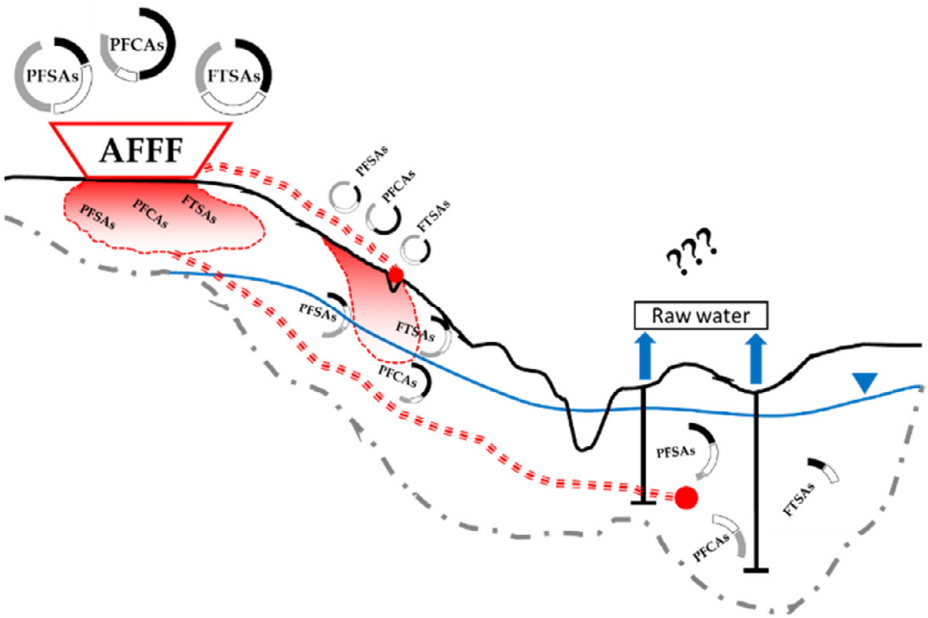

Figure 12. Conceptualisation of the PFAS release, transport, and distribution at the site surrounding the aquatic environment (Figure 4 in Paper III).

According to former personnel, the exercise included an initial blast (on-vehicle) of the rescued aircraft with AFFF. Consequently, when the simulated aircraft fire is partially supressed, a secondary suppression was conducted (off-vehicle) with targeted application of AFFF. It was also suggested (by former personnel), that fire training sessions were possibly followed by clean-up stages where the aircraft crash simulation area was flushed with water. It is therefore assumed, that an individual training session could contribute to generation of a substantial amount of liquid. Thus, including AFFF release, AFFF dissociation and possible post-application of water, the mass generated during the exercise session is considered sufficient for possible PFAS transport with surface runoff. The transport and distribution with runoff, however, are affected by topographical features and soil saturation conditions of the area surrounding the FTF. Furthermore, the PFAS transport with surface runoff may have been affected by re-direction of surface flows with the drainage system at FTF. However, very limited information is available on the drainage operation period as well as its transport capacity. It is presumed that the PFAS transport with surface runoff and following distribution processes are associated with hydrological processes of much longer response time. PFAS distribution associated with infiltration process and transport in unsaturated soil, is considered as primary contributor to PFAS accumulation in porous media, as well as a shift in PFAS composition prior to further advective transport. However, due to complex interaction mechanisms in the porous media, the PFAS transport in

unsaturated soil is difficult to predict with certainty, not least due to limited data available on the contaminant emission.

The advective stage of the PFAS transport is primarily subject to transport in dissolved state (with groundwater). Although, the PFAS transport is assumed to primarily occur in soil of high permeability and mostly connected to free-water mobility, the retardation/sorption process is relevant to certain soil fractions and compositions. Ultimately, the PFAS sorption and transport in aqueous-solid, solid-air, and aqueous-air interfaces are complicated and not well studied processes. The PFAS sorption/interaction can be affected by mineral composition of the heterogeneous media as well porosity and pore-size distribution (Johnson et al., 2007; Jeon et al., 2011; Weber et al., 2017; Pereira et al., 2018). Further investigation is required to a better understand the PFAS distribution in soil and groundwater.

Further PFAS transport was primarily connected to groundwater extraction, processing, and distribution with drinking water. Since water treatment, prior to plant modification, was restricted to treatment barriers insensitive to PFAS, the drinking water is assumed to have been contaminated for an extended period.

PFAS treatment (UVC/VUV)

The experiments on UVC/VUV induced PFAS removal in water (ultrapure water) were conducted in the set of experimental trials with different exposure conditions (i.e., hydraulic residence time, different PFAS combinations and exposure times) (Table 7). The UV output (emission) was kept constant throughout the experiments; UV transmission was primarily controlled by the immersion sleeve material with (calculated) 0.067 W mm^{-1} at 254 nm and 0.002 W mm^{-1} at 185 nm delivered to the aqueous phase. For better representation of the actual exposure (contact) times and comparison between experimental trials, corresponding sampling times were accordingly converted and expressed as (nondimensional) treatment cycles.

In trials with negative blank samples (A1) the occurrence of potential degradation and transformation products produced by the system material (during exposure to UVC/VUV) was validated. The system was set operating with UVC/VUV exposure for 10 hrs prior to consequent sampling during the 300 min exposure period. There was no PFAS contamination observed in samples taken during the studied exposure time, except for single detection of 6:2 FTSA at <10 ng L^{-1}. The experimental quantification limits were adjusted accordingly (Paper IV, Table S2 in supplementary materials).

Table 7. Experimental trials and corresponding sampling conditions (Table 1 in Paper IV).
[1] hydraulic residence time (HRT), [2] corresponding blank sample trials, [3] no exposure to UVC/VUV

Trial	Spike	Exposure time	Sample type	System volume	HRT[1]
A1[2]	No spike	300 min	negative blank	1.1L	13.2 min
B1[2]	10:2 FTSA, 8:2 FTSA, 6:2 FTSA, FOSA and FOSAA	60 min[3]	positive blank		6.6 min
B2[2]					
B1		300 min	treatment sample		
B2					
C1[2]	PFBS, PFHxS, PFOS, PFHpA, PFOA and PFNA	45 min[3]	positive blank		13.2 min
C2[2]		60 min[3]			
C1		300 min	treatment sample		
C2					
C3[2]	PFBS, PFHxS, PFOS, PFOA and PFNA	15 min[3]	positive blank	0.8 L	9.6 min
C4[2]		15 min[3]			
C3		120 min	treatment sample		
C4		600 min			

Removal of perfluoro-sulfonamides (FOSA and FOSAA) was studied in experimental trials B1 and B2. The equilibrated concentrations were measured in positive blank trials (taken post 10 hrs equilibration period) and estimated as 88±9 (n=6) ng L^{-1} and 92±10 (n=5) ng L^{-1} for FOSA, and 563±50 (n=6) and 101±11 (n=5) ng L^{-1} ng L^{-1} for FOSAA in experimental trials B1 and B2, respectively (Paper IV, tables S4 and S6 in supplementary materials).

In the measured concentrations of both FOSA and FOSAA, there was an increase observed in beginning of the treatment process, followed by degradation in 20 treatment cycles for FOSA and 10 treatment cycles for FOSAA, respectively (Figure 13).

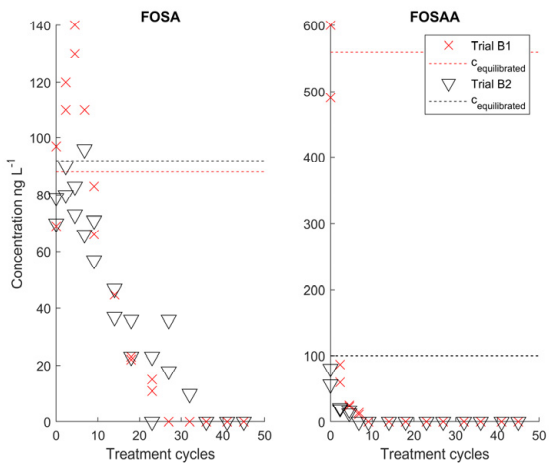

Figure 13. UVC/VUV induced reduction in measured FOSA and FOSA levels (experimental trials B1 and B2) (Figure 2 in Paper IV).

Reduction occurred with estimated degradation half times of 0.96 hrs (k= -0.0002 at R^2=0.82) for FOSA and 0.17 hrs (k= -0.0011 at R^2=0.64) for FOSAA, respectively.

Removal of the fluorotelomer sulfonates (including 10:2 FTSA, 8:2 FTSA and 6:2 FTSA) was studied in experimental trials B1 and B2. The measured equilibrated concentrations were 31±6 (n=6) ng L^{-1} and 20±5 (n=5) ng L^{-1} for 10:2 FTSA, 835±109 (n=6) ng L^{-1} and 496±52 (n=5) ng L^{-1} for 8:2 FTSA and 1183±133 (n=6) ng L^{-1} and 1098±74 (n=5) ng L^{-1} for 6:2 FTSA, respectively (Paper IV, Table S4 and S6 in supplementary materials).

For fluorotelomer sulfonates, the variation in measured concentrations showed a common pattern of identical increase above the equilibrated baseline concentrations as observed with perfluoro-sulfonamides (Figure 13). Reduction occurred within about 20 treatment cycles for 10:2 FTSA and 8:2 FTSA, and about 10 treatment cycles for 6:2 FTSA (Figure 14). The observed degradation half times were estimated as 0.96 hrs (k= -0.0002 at R^2=0.68 and R^2=0.77) for 10:2 FTSA and 6:2 FTSA, followed by 0.64 hrs (k= -0.0003 at R^2=0.85) for 8:2 FTSA.

In samples corresponding to treatment trials B1 and B2, respectively, occurrence of PFCAs was observed with concentrations of 41±21 (n=8) ng L^{-1} and 63±43 (n=12) ng L^{-1} for PFHpA, 16±6 (n=4) ng L^{-1} for PFHxA, and 37±30 (n=12) ng L^{-1} and 57±46 (n=13) ng L^{-1} for PFOA. Production of PFCAs occurred in the beginning of the treatment process, followed by removal within approximately 18 treatment cycles (Paper IV, Table S4 and S6 in supplementary materials).

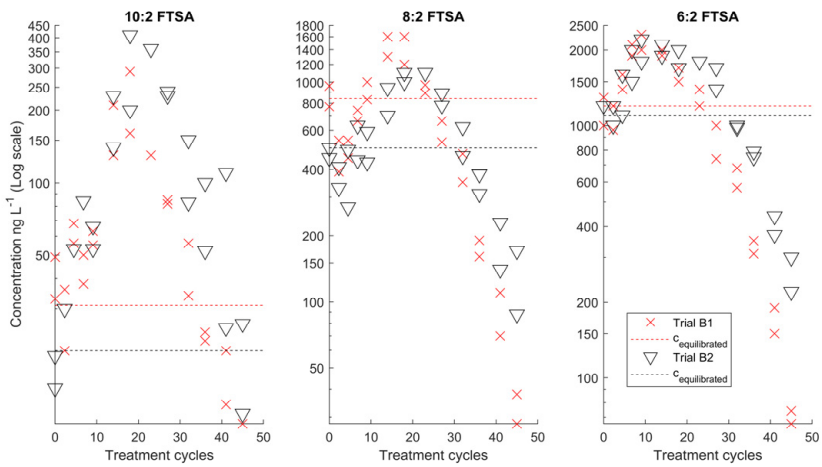

Figure 14. UVC/VUV induced reduction in measured 10:2 FTSA, 8:2 FTSA and 6:2 levels (experimental trials B1 and B2) (Figure 3 in Paper IV).

Removal of perfluoroalkyl carboxylates was studied in experimental trials C1, C2, C3, and C4. These included PFHpA (C1 and C2), PFOA (C1 trough C4) and PFNA (C1 trough C4) (Paper IV, Table S8, S10, S12, and S14 in supplementary materials).

For PFOA and PFNA, there was no significant fluctuation observed between equilibrated concentrations and concentration at the start of the treatment process (Figure 15). Reduction occurred simultaneously with exposure to UVC/VUV followed by drop from the initial equilibrated concentrations as 3314±177 (n=7), 1700±141 (n=5), 983±83 (n=4) and 2100±82 (n=4) ng L^{-1} for PFOA (C1 trough C4); 3300±183 (n=7), 1760± 230 (n=5), 923±34 (n=4), and 1975±50 (n=4) ng L^{-1} for PFNA (C1 through C4) (Paper IV, tables S7, S9, S11, and S13 in supplementary materials). For PFHpA, the initial treatment process concentrations were exceeding the equilibrated (baseline) concentrations (as 40±2 (n=7) and 18±2 (n=5) ng L^{-1} in trials C1 and C2, respectively).

Removal of PFCAs (including PFHpA, PFOA, and PFNA) occurred within approximately 10 treatment cycle. The observed degradation halftimes were estimated as 0.64 hrs (k= -0.0003 at R^2=0.62) for PFHpA (C1 and C2), 0.24–0.27 hrs (k= -0.0007 at R^2=0.93 (C1 and C2) and k= -0.0008 at R^2=0.97 (C3 and C4)) for PFOA and 0.21 hrs (k= -0.0009 at R^2=0.96 (C1 and C2), and at R^2=0.94 (C3 and C4)) for PFNA.

PFHxA occurrence (30±11 (n=4) and 18±3 (n=4) ng L^{-1}) was observed during experimental trials C1 and C2, respectively; PFHxA was degraded within the first 5 treatment cycles.

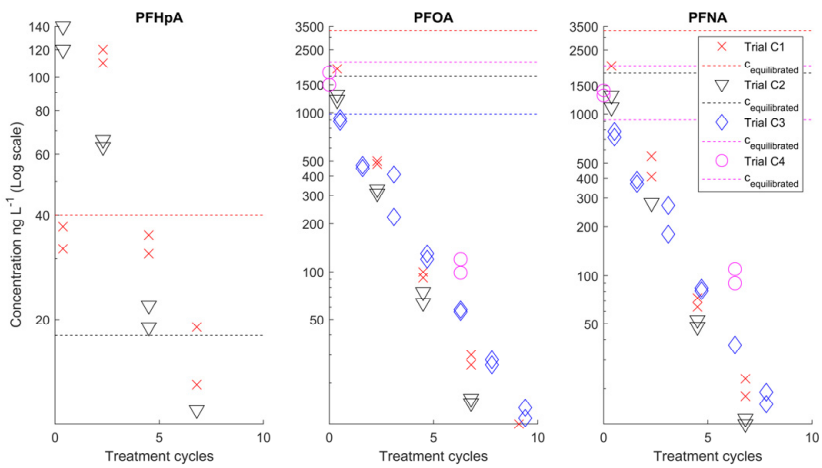

Figure 15. UVC/VUV induced reduction in measured PFHpA, PFOA, and PFNA levels (experimental trials C1, C2, C3, and C4) (Figure 4 in Paper IV).

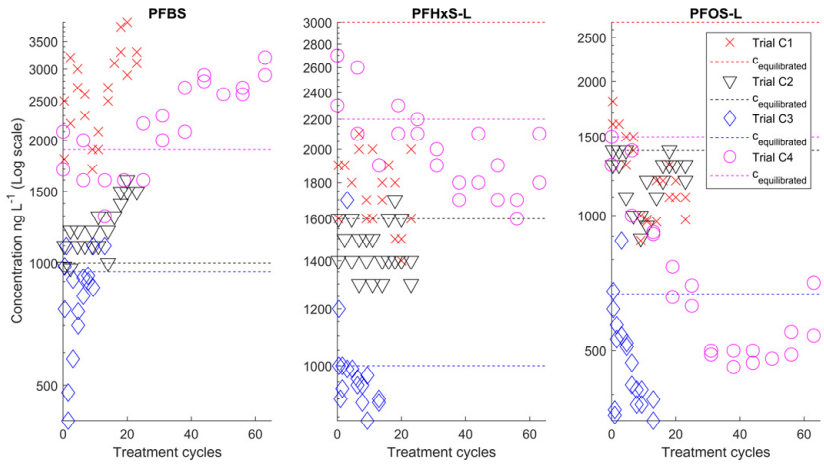

Figure 16. UVC/VUV induced variation in measured PFBS, PFHxS-L, and PFOS-L levels (experimental trials C1, C2, C3, and C4) (Figure 5 in Paper IV).

In experimental trials C1, C2, C3, and C4, the variation in concentration of PFBS, PFHxS, and PFOS showed no significant regression (Figure 16). For PFHxS-L, the measured concentrations remained fluctuating about measured baseline concentrations (1686±421 (n=22), 1455±114 (n=22), 996±192 (n=18) and 2014±285 (n=22) ng L^{-1} in trials C1 through C4, respectively) with no reduction during the studied exposure periods; the variation of PFHxS-B concentrations remained identical (304±77 (n=22) and 229±18 (n=22) in trials C1 and C2) (Paper IV, tables S8, S10, S12, and S14 in supplementary materials).

There was no reduction observed for PFOS-L in experimental trials C1, C2, and C3; with measured average concentrations of 1195±371 (n=22), 1202±160 (n=22) and 488±137 (n=18) ng L^{-1}, respectively (Figure 16). However, in trial C4, corresponding to 63 treatment cycles (600 min exposure period), there was a decrease in concentrations observed for PFOS-L with reduction from measured baseline concentration (1500±115 (n=4) ng L^{-1}) with mean of 726 and average (mean) absolute deviation (MAD) of 247 (n=22). Reduction was also observed for PFOS-B in experimental trials C1 and C2 with average concentrations of 491±173 MAD (n=22) and 415 ±85 MAD (n=22) ng L^{-1} (Figure 17).

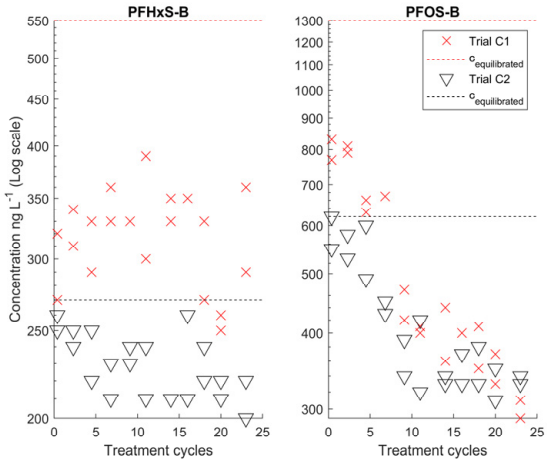

Figure 17. UVC/VUV induced variation in measured PFHxS-B, and PFOS-B levels (experimental trials C1, C2, C3, and C4) (Figure 6 in Paper IV).

For PFBS, there was an increase from the measured baseline levels (C1 through C4). PFBS production (k=0.00004 at R^2=0.64) appeared to begin with treatment and continued during exposure to UVC/VUV.

Regarding exposure conditions, the system design was optimized for exposure at 185 nm wavelength, using a relatively weak radiation source in form of a low-pressure mercury lamp. However, further investigation is necessary to confirm the actual UV dose, photon fluxes (at corresponding wavelengths), radial flux distribution, and radical generation. There was no background contamination found in negative blank sample (trial A1) evaluation. Hence, possible PFAS emission from the system (during UVC/VUV exposure) is considered insignificant and the system is considered clean in relation to PFAS analysis. Materials were selected to minimize the PFAS losses due to sorption. As was observed in trials B1 and B2, PFAS interaction with system materials might cause significant fluctuation in the measured concentrations. PFAS distribution in the system most likely took place during the equilibration stage, when sufficient time was given for relaxation of the molecules on system surfaces. The layer formation on the surfaces was further disrupted with initiation of the treatment, causing reversion to the dissolved state. Distribution of long-chain zwitterionic perfluoro-sulfonamides and fluorotelomer sulfonates in the system is suggested to occur due to intermolecular interactions with quartz glass (sleeve) and native PTFE of the system body. Proper material selection can be of high importance for the upscaling consideration.

Conducted PFAS removal trials (B1, B2, C1, C2, C3, and C3) showed that UVC/VUV induced degradation was achieved at greater level for perfluoroalkyl carboxylates and perfluoro-sulfonamides, followed by fluorotelomer sulfonates.

PFAS degradation rates followed the order as FOSAA > PFNA > PFOA > 8:2 FTSA ≈ PFHpA ≈ 10:2 FTSA ≈ 6:2 FTSA ≈ FOSA. There was no apparent connection between PFAS degradation rates and chain length observed. Furthermore, in trials with perfluoro-sulfonamides, fluorotelomer sulfonates and perfluoroalkyl carboxylates, initial PFAS concentrations seem to have no effect on degradation rates. This, possibly indicates that studied treatment is a transport-limited process (limited by the rate by which PFAS solution reaches the reaction area in the chamber).

Degradation of PFSAs was found insufficient within the studied exposure (treatment) periods, except for observed reduction in PFOS-B levels. Further investigation is required for optimisation of the PFSAs treatment conditions and evaluation of degradation rates.

In relation to removal of perfluoro-sulfonamides, fluorotelomer sulfonates, perfluoroalkyl carboxylates, and perfluoroalkane sulfonates, it appeared that compounds containing protonated (non-fluorinated) moiety in the structure (PFCAs, FTSAs) show greater sensitivity to treatment. This is also relevant for PFAS with sulfonamide in the functional group (as perfluoro-sulfonamides). Compounds with sulfonate in functional group exhibit persistence to treatment. It is suggested that oxygen saturation of the sulfonate (in functional group) might be a factor in persistence of PFSAs to degradation. For further discussion, however, it is necessary to verify the reaction chain behind the removal process and confirm whether decomposition occurs due to direct excitation by UVC/VUV or/and secondary impact of the generated radicals. UVC/VUV-induced degradation of PFAS is most likely initiated with decomposition of the functional group, followed by consequent degradation of the fluorinated chain (Ochiai et al., 2011b; Giri et al., 2012).

Presence of transformation products was observed in all trials. In trials with perfluoro-sulfonamides (FOSA and FOSAA) and fluorotelomer sulfonates (10:2 FTSA, 8:2 FTSA and 6:2 FTSA) (B1 and B2), occurrence of PFCAs (PFOA, PFHpA, PFHxA) was connected to degradation of the octanoic-PFAS. The initial octanoic fluorotelomer and/or sulfonamide can possibly transform into sole perfluoroalkyl carboxylate (PFOA) followed by further degradation to PFHxA and PFHpA. With PFCAs and PFSAs (C1 and C2), occurrence of PFHxA can be connected to degradation of the initial PFCAs of longer chain-length. However, further investigation with individual PFAS is required to confirm the exact degradation chain. Furthermore, verification of the degradation (i.e., mineralization) is necessary. Measurements of CO2, fluoride (F^-), total organic fluorine (TOF), as well as measurement of potential fluorinated gasses in the gas phase, could be applied to confirm the PFAS degradation products.

Conclusions

PFAS concentrations were measured in the water samples collected from Lake L (and pond P) (Paper I), Lake S (Paper II) and groundwater (Paper III).

In **surface water** samples (L (P) and S) detected PFAS compositions were identical to these reported for other contaminated sites (restrictive to PFAS-AFFF). Contamination levels were represented by PFCAs, PFSAs, and FTSAs, thus indirectly connecting to the PFAS-AFFF origin of contamination. For both L and S, it was difficult to conclude the exact contamination path. Thus, until water exchange and transport conditions are properly established, PFAS concentration in water samples is not considered as a direct indictor of the overall contamination levels quantitively, but only qualitatively. Furthermore, the PFAS-AFFF emission rates can have an impact on observed levels. Nevertheless, at both studied locations PFAS contamination was subject to a historical PFAS-AFFF application.

Identically, the **groundwater contamination** (Paper III) was connected to PFAS-AFFF. Profiling of the PFAS composition was sufficiently indicative to determine the respective PFAS-AFFF formulations. Based on measured concentrations and compositions, PFAS distribution, as well as possible concentration gradients, were suggested. Thus, the overall contamination levels in groundwater could be estimated; this is of course with assumption on rather conservative mass transfer. Yet, the sorption and transport processes in the corresponding domain can have an impact on observed PFAS concentrations.

Moreover, on the basis of the assessment, the analytical methods are of importance. PFAS analysis was carried out by means of MS/MS. Used method is considered precise and reliable, furthermore, internal standards were used to fortify the measurements. However, in the performed target analysis, detected compositions might not be fully representative.

A **sediment core analysis** approach was implemented for Lake L and Lake S (Paper I and II). With combination of MS/MS and **radioisotope analysis** (^{210}Pb/^{226}Ra), the core analysis was sufficient to evaluate the contamination history of individual exposed recipient (Lake L). Thus, possible PFAS accumulation rates and fluxes were determined; these in relation to the lake contamination. PFAS accumulation period was estimated as 1994–2009; this with the highest PFAS flux of 12 μg m^{-2} yr^{-1} by year 2009. However, provided estimates are unidimensional, thus better understanding of the horizontal transport of the PFAS plume, as well sediment

resuspension, are necessary for further extrapolation. Thus, additional sampling and analysis are imperative for a complete picture.

For the Lake S (Paper II), the core analysis was implemented for same purpose, however, the method combination was not successful. This most likely due to sedimentation dynamics of the lake, as well as analytical difficulties.

The **sediment core analysis** was further extended to combination with **XRF** analysis. Thus, the influence of the sediment specific characteristics on PFAS distribution in sediment was studied. A correlation between PFAS concentrations (PFCAs and PFSAs) and sediment inorganic content (lead, arsenic, iron, titanium, and sulphur) was found. This is of importance as a validation of the electrostatic interaction with the mineral content of the media. Furthermore, the solid-state intrinsic properties can be correlated with PFAS dissociation to the aqueous phase. Moreover, the fact that PFAS distribution is affected by the inorganic content representing <5% of the bulk media, the hydrophobic interaction with organic matter might be a driving distribution factor. This is can be of importance for the sorption and transport considerations.

Field-derived **distribution predictors** (K_d and K_{OC}) (Papers I and II) were in general agreement with previously reported for various sediments, within a certain variation. Field-derived K_d and K_{OC} predictors are of importance in the PFAS transport assessment. However, due to limited knowledge on PFAS distribution, the universal cross-site application should be considered with a precaution. Perhaps, taken as a site- and media- specific, as well as with local equilibrium conditions properly established, implementation of K_d and K_{OC} in the PFAS transport assessment can be considered with level of confidence.

Detailed assessment of the **emission source** was conducted for the site in Ronneby, Sweden (Paper III). The PFSAs based PFAS-AFFF and PFCAs/FTSAs based PFAS-AFFF were indicated as an emission contributor. Furthermore, traces of perfluoroalkane sulphonamides substances, such as FOSA and MeFOSA, were linked to PFAS synthesis processes and indirectly connected to PFAS-AFFF origin. However, conducted identification was primarily based on measured PFAS composition in groundwater, and therefore possibly neglecting PFAS that are affected by transport and retention.

Analysis of potential PFAS release (production) scenarios was conducted by means of Monte Carlo simulations. These considered individual fire-training sessions and annual emission scenarios. For **individual fire-training session** scenarios, possible variation in the AFFF stock solution composition, surfactant composition (PFAS content), AFFF solution, and equipment utilisation were considered. PFAS emission from an individual training was estimated as [1.4 <11.5±5.7 <43.7] kg per session. The annual emissions were estimated as [11 <401±233 <1125 kg yr^{-1}]; this corresponding to [2 <35±20 <96] individual fire-training sessions per year. **Annual emission scenarios** were evaluated based on fire-training exercise routines

suggested by former personnel (including 2-6 individual sessions per day, 1-5 training days, with 1-5 occurrences per year). However, the annual emission scenarios are restricted to the evaluated population with a rather limited sample, further improvements are necessary. Furthermore, PFAS-AFFF composition were not considered at this stage.

In the trials with **UVC/VUV induced treatment** (Paper IV), removal of the perfluoro-sulfonamides (FOSA and FOSAA), fluorotelomer sulfonates (10:2 FTSA, 8:2 FTSA and 6:2 FTSA), perfluoroalkyl carboxylates (PFHpA, PFOA and PFNA), and perfluoroalkane sulfonates (PFBS, PFHxS-L, PFHxS-B, PFOS-L and PFOS-B) was studied in laboratory conditions. In relation to individual PFAS, method evaluation showed removal efficiency in the order FOSAA > PFNA > PFOA > 8:2 FTSA ≈ PFHpA ≈ 10:2 FTSA ≈ 6:2 FTSA ≈ FOSA. No significant reduction was observed for PFSAs. No apparent connection between PFAS degradation rates and chain length was observed. The initial PFAS concentration is suggested to have no effect on the removal rates. Further investigation is certainly necessary.

To further elaborate, with the degradation chain studied and an actual degradation (i.e., mineralization) verified, suggested technique can have a substantial potential in PFAS treatment for drinking water. The method performance with FASAs, FOSAAs, FASEs, FTSAs, and PFCAs can be very useful as a barrier and used in a combination with, for example, AIX resins.

Delimitations and Future work

In present thesis, investigations have been carried out in association with the epidemiological study on human exposure to PFAS conducted by Lund University and University of Gothenburg. With the given objective to reconstruct the PFAS contamination levels in drinking water during the last decades (in Ronneby), an exciting and yet challenging journey of trials and errors has evolved. Several different approaches have been implemented, leaving some questions answered and perhaps more arisen. Like many other research projects, this study encountered difficulties with method performance and had limitations related to resources and time. As mentioned earlier, not all indicial objectives were fully addressed, and not all the outcomes were reported (as shown in Figure 1). In the present chapter, limitations of the work, as well as aspects of further development and future work will be extended.

Regarding PFAS composition detected in water and sediment samples, conducted analyses (MS/MS) can provide sufficient resolution, however, detected composition is limited to method. Thus, PFAS composition and related concentrations may not represent the actual contamination in full. PFAS analysis can be fortified by combination with the methods like TOF analysis, high resolution mass spectrometry (HRMS), total oxidable precursors (TOP) assay, and fast atom bombardment mass spectrometry (FAB-MS). This can improve the representation of PFAS composition, facilitate identification of the origin (PFAS-AFFF formulation), and not least help with assessment of the contaminant distribution.

Understanding of the PFAS sorption and transport mechanisms is important for assessment of the overall transport processes. Association of PFAS with the solid phase is a complex process that is impacted by intermolecular interaction with media surfaces and structure. It will, therefore, be interesting to further continue with analysis of PFAS distribution in connection to intrinsic characteristics of media. Detailed analysis of the media (i.e., soil and sediment) composition and porosity vs PFAS partitioning in pore water and water, can be provide important insights. This data can be essential in determining the likelihood of PFAS retention in certain soil fractions and compositions.

In the analysis of PFAS-AFFF emission, provided estimates were restricted by both calculation limitations and knowledge of AFFF application scenarios and history. Method performance can be improved by accordingly adjusting the variation

boundaries and extending the overall simulation capacity. Furthermore, as a next step, introduction of the PFAS-AFFF formulation scenarios can provide a range of possible PFAS emission estimates. Following outcomes can be useful in understanding of the overall pollution and contaminant transport conditions.

In appended Paper III, attempts were made regarding assessment of PFAS transport and redistribution in water supply. However, due to limited information available on PFAS emission and distribution in soil, a relevant analysis was not possible at this stage. An alternative was later considered with implementation of a probabilistic approach on PFAS transport and redistribution in water supply system. This, coupled with PFAS-AFFF emission estimates above, and including transport with run-off, infiltration/retention, advective transport, groundwater extraction, and water treatment plant sub-models. It is, therefore, necessary to continue with further model development and evaluation. There are perhaps a several steps remaining in addressing the initial project objective. Given the difficulties with assessment of the PFAS contamination in a historical context, suggested approach can be useful in assessment of other contaminated sites.

In the treatment trials with UVC/VUV, PFAS removal was studied in laboratory conditions. Thus, it is necessary to evaluate the method performance with different environmental matrices. Furthermore, as mentioned earlier, verification of the degradation (i.e., mineralization) and degradation chain are of high importance.

Removal of FASAs, FOSAAs, FASEs, FTSAs, and PFCAs can be useful in combination with other treatment methods (GAC, AIX resins, and other sorbents). This can provide a selective reduction in PFAS mass, in particular for zwitterionic PFAS and various structural isomers, thus fortifying the coupled method performance and efficiency. With tailored implementation in the treatment train, suggested methods can also act a barrier for pharmaceuticals and related organic substances.

In the context of drinking water, there are numerous treatment methods being developed. These can be as straightforward as GAC, NF, AIX resins, and their combinations, or incorporating rather advanced, and perhaps exotic, processes behind the treatment line. However, finding of an integrated and cost-efficient method or method combination, is yet a subject to further research and development. The overall quality of the treated water and composition of the treated PFAS can have an impact on the method performance in one way or another. Thus, source water related (or site-specific) verifications are important prior to further method implementation; not least prior to upscaling considerations and deployment in the full-scale drinking water treatment.

References

Ahrens, L., Bundschuh, M., 2014. Fate and Effects of Poly- and Perfluoroalkyl Substances in the Aquatic Environment: A Review. Environ Toxicol Chem 33, 1921-1929.

Ahrens, L., Norstrom, K., Viktor, T., Cousins, A.P., Josefsson, S., 2015. Stockholm Arlanda Airport as a source of per- and polyfluoroalkyl substances to water, sediment and fish. Chemosphere 129, 33-38.

Ahrens, L., Taniyasu, S., Yeung, L.W.Y., Yamashita, N., Lam, P.K.S., Ebinghaus, R., 2010. Distribution of polyfluoroalkyl compounds in water, suspended particulate matter and sediment from Tokyo Bay, Japan. Chemosphere 79, 266-272.

Ahrens, L., Yamashita, N., Yeung, L.W.Y., Taniyasu, S., Horii, Y., Lam, P.K.S., Ebinghaus, R., 2009. Partitioning Behavior of Per- and Polyfluoroalkyl Compounds between Pore Water and Sediment in Two Sediment Cores from Tokyo Bay, Japan. Environ Sci Technol 43, 6969-6975.

Ahrens, L., Yeung, L.W.Y., Taniyasu, S., Lam, P.K.S., Yamashita, N., 2011. Partitioning of perfluorooctanoate (PFOA), perfluorooctane sulfonate (PFOS) and perfluorooctane sulfonamide (PFOSA) between water and sediment. Chemosphere 85, 731-737.

Alsmeyer, Y., Childs, W., Flynn, R., Moore, G., Smeltzer, J., 1994. Electrochemical Fluorination and Its Applications. pp. 121-143.

Andersen, M.E., Butenhoff, J.L., Chang, S.C., Farrar, D.G., Kennedy, G.L., Jr., Lau, C., Olsen, G.W., Seed, J., Wallace, K.B., 2008. Perfluoroalkyl acids and related chemistries--toxicokinetics and modes of action. Toxicol Sci 102, 3-14.

Andersson, E.M., Scott, K., Xu, Y., Li, Y., Olsson, D.S., Fletcher, T., Jakobsson, K., 2019. High exposure to perfluorinated compounds in drinking water and thyroid disease. A cohort study from Ronneby, Sweden. Environ Res 176, 108540.

Appleman, T.D., Higgins, C.P., Quinones, O., Vanderford, B.J., Kolstad, C., Zeigler-Holady, J.C., Dickenson, E.R.V., 2014. Treatment of poly- and perfluoroalkyl substances in US full-scale water treatment systems. Water Res 51, 246-255.

Armitage, J.M., Cousins, I.T., Buck, R.C., Prevedouros, K., Russell, M.H., MacLeod, M., Korzeniowski, S.H., 2006. Modeling global-scale fate and transport of perfluorooctanoate emitted from direct sources. Environ Sci Technol 40, 6969-6975.

Armitage, J.M., Schenker, U., Scheringer, M., Martin, J.W., MacLeod, M., Cousins, I.T., 2009. Modeling the Global Fate and Transport of Perfluorooctane Sulfonate (PFOS) and Precursor Compounds in Relation to Temporal Trends in Wildlife Exposure. Environ Sci Technol 43, 9274-9280.

Awad, E., Zhang, X.M., Bhavsar, S.P., Petro, S., Crozier, P.W., Reiner, E.J., Fletcher, R., Tittemier, S.A., Braekevelt, E., 2011. Long-Term Environmental Fate of Perfluorinated Compounds after Accidental Release at Toronto Airport. Environ Sci Technol 45, 8081-8089.

Backe, W.J., Day, T.C., Field, J.A., 2013. Zwitterionic, Cationic, and Anionic Fluorinated Chemicals in Aqueous Film Forming Foam Formulations and Groundwater from US Military Bases by Nonaqueous Large-Volume Injection HPLC-MS/MS. Environ Sci Technol 47, 5226-5234.

Baum, E., 1997. Chemical Property Estimation: Theory and Application.

Bengtsson, L., Westerstrom, G., 1992. Urban Snowmelt and Runoff in Northern Sweden. Hydrolog Sci J 37, 263-275.

Buck, R.C., Franklin, J., Berger, U., Conder, J.M., Cousins, I.T., de Voogt, P., Jensen, A.A., Kannan, K., Mabury, S.A., van Leeuwen, S.P., 2011. Perfluoroalkyl and polyfluoroalkyl substances in the environment: terminology, classification, and origins. Integr Environ Assess Manag 7, 513-541.

Busch, J., Ahrens, L., Sturm, R., Ebinghaus, R., 2010. Polyfluoroalkyl compounds in landfill leachates. Environ Pollut 158, 1467-1471.

Carter, K.E., Farrell, J., 2008. Oxidative destruction of perfluorooctane sulfonate using boron-doped diamond film electrodes. Environ Sci Technol 42, 6111-6115.

Chen, H., Zhang, C., Yu, Y.X., Han, J.B., 2012. Sorption of perfluorooctane sulfonate (PFOS) on marine sediments. Mar Pollut Bull 64, 902-906.

Colosi, L.M., Pinto, R.A., Huang, Q., Weber, W.J., Jr., 2009. Peroxidase-mediated degradation of perfluorooctanoic acid. Environ Toxicol Chem 28, 264-271.

Cousins, I.T., Vestergren, R., Wang, Z.Y., Scheringer, M., McLachlan, M.S., 2016. The precautionary principle and chemicals management: The example of perfluoroalkyl acids in groundwater. Environ Int 94, 331-340.

Deng, S., Nie, Y., Du, Z., Huang, Q., Meng, P., Wang, B., Huang, J., Yu, G., 2015. Enhanced adsorption of perfluorooctane sulfonate and perfluorooctanoate by bamboo-derived granular activated carbon. J Hazard Mater 282, 150-157.

Dickenson, E., Higgins, C., 2016. Treatment Mitigation Strategies for Poly- and Perfluoroalkyl Substances. Water Research Foundation Project #4322.

Dombrowski, P.M., Kakarla, P., Caldicott, W., Chin, Y., Sadeghi, V., Bogdan, D., Barajas-Rodriguez, F., Chiang, S.-Y., 2018. Technology review and evaluation of different chemical oxidation conditions on treatability of PFAS. Remed J 28, 135-150.

EFSA, 2020. European Food Safety Authority: Risk to human health related to the presence of perfluoroalkyl substances in food, web source: https://doi.org/10.2903/j.efsa.2020.6223 (accessed on 2021-09-02).

EPA, U.S., 1999. Understanding Variation in Partition Coefficient, Kd, Values. United States Environmental Protection Agency.

EPA, U.S., 2007. Field portable X-Ray Fluorescence Spectrometry for the determination of elemental concentrations in soil and sediment. United States Environmental Protection Agency.

Espan, V.A.A., Mallavarapu, M., Naidu, R., 2015. Treatment technologies for aqueous perfluorooctanesulfonate (PFOS) and perfluorooctanoate (PFOA): A critical review with an emphasis on field testing. Environ Technol Inno 4, 168-181.

EU, 2020. Directive (EU) 2020/2184 of the European parliament and of the Council of 16 December 2020 on the quality of water intended for human consumption, web source: https://eur-lex.europa.eu/legal-content/EN/TXT/PDF/?uri=CELEX:32020L2184&from=EN (accessed on 2021-09-02).

F17, 2020. F17, web source: https://www.forsvarsmakten.se/sv/organisation/blekinge-flygflottilj-f-17/ (accessed on 2020-11-27).

Filipovic, M., Berger, U., McLachlan, M., 2013. Mass Balance of Perfluoroalkyl Acids in the Baltic Sea. Environ Sci Technol 47, 4088-4095.

Filipovic, M., Laudon, H., McLachlan, M., Berger, U., 2015a. Mass Balance of Perfluorinated Alkyl Acids in a Pristine Boreal Catchment. Environ Sci Technol 49, 12127-12135.

Filipovic, M., Woldegiorgis, A., Norstrom, K., Bibi, M., Lindberg, M., Osteras, A.H., 2015b. Historical usage of aqueous film forming foam: a case study of the widespread distribution of perfluoroalkyl acids from a military airport to groundwater, lakes, soils and fish. Chemosphere 129, 39-45.

Franke, V., McCleaf, P., Lindegren, K., Ahrens, L., 2019. Efficient removal of per- and polyfluoroalkyl substances (PFASs) in drinking water treatment: nanofiltration combined with active carbon or anion exchange. Environ Sci-Wat Res 5, 1836-1843.

Franke, V., Ullberg, M., McCleaf, P., Wålinder, M., Köhler, S.J., Ahrens, L., 2021. The Price of Really Clean Water: Combining Nanofiltration with Granular Activated Carbon and Anion Exchange Resins for the Removal of Per- And Polyfluoralkyl Substances (PFASs) in Drinking Water Production. ACS ES&T Water 1, 782-795.

Giesy, J.P., Kannan, K., 2001. Global distribution of perfluorooctane sulfonate in wildlife. Environ Sci Technol 35, 1339-1342.

Giri, R.R., Ozaki, H., Okada, T., Taniguchi, S., Takanami, R., 2012. Factors influencing UV photodecomposition of perfluorooctanoic acid in water. Chem Eng J 180, 197-203.

Gobelius, L., Hedlund, J., Durig, W., Troger, R., Lilja, K., Wiberg, K., Ahrens, L., 2018. Per- and Polyfluoroalkyl Substances in Swedish Groundwater and Surface Water: Implications for Environmental Quality Standards and Drinking Water Guidelines. Environ Sci Technol 52, 4340-4349.

Gobelius, L., Persson, C., Wiberg, K., Ahrens, L., 2019. Calibration and application of passive sampling for per- and polyfluoroalkyl substances in a drinking water treatment plant. J Hazard Mater 362, 230-237.

Gramstad, T., Haszeldine, R.N., 1957. 512. Perfluoroalkyl derivatives of sulphur. Part VI. Perfluoroalkanesulphonic acids CF3·[CF2]·SO3H (n= 1—7). J Chem Soc, 2640-2645.

Greaves, A.K., Letcher, R.J., 2013. Linear and branched perfluorooctane sulfonate (PFOS) isomer patterns differ among several tissues and blood of polar bears. Chemosphere 93, 574-580.

Hellsing, M.S., Josefsson, S., Hughes, A.V., Ahrens, L., 2016. Sorption of perfluoroalkyl substances to two types of minerals. Chemosphere 159, 385-391.

Higgins, C.P., Luthy, R.G., 2006. Sorption of perfluorinated surfactants on sediments. Environ Sci Technol 40, 7251-7256.

Houde, M., Czub, G., Small, J.M., Backus, S., Wang, X., Alaee, M., Muir, D.C., 2008. Fractionation and bioaccumulation of perfluorooctane sulfonate (PFOS) isomers in a Lake Ontario food web. Environ Sci Technol 42, 9397-9403.

Houde, M., Martin, J.W., Letcher, R.J., Solomon, K.R., Muir, D.C.G., 2006. Biological monitoring of polyfluoroalkyl substances: A review. Environ Sci Technol 40, 3463-3473.

Hu, X.D.C., Andrews, D.Q., Lindstrom, A.B., Bruton, T.A., Schaider, L.A., Grandjean, P., Lohmann, R., Carignan, C.C., Blum, A., Balan, S.A., Higgins, C.P., Sunderland, E.M., 2016. Detection of Poly- and Perfluoroalkyl Substances (PFASs) in US Drinking Water Linked to Industrial Sites, Military Fire Training Areas, and Wastewater Treatment Plants. Environ Sci Tech Let 3, 344-350.

Jensen, A., 2010. Draft guidance document on alternatives to perfluorooctane sulfonate and its derivatives. Stockholm Convention.

Jeon, J., Kannan, K., Lim, B.J., An, K.G., Kim, S.D., 2011. Effects of salinity and organic matter on the partitioning of perfluoroalkyl acid (PFAs) to clay particles. J Environ Monit 13, 1803-1810.

Johnson, R.L., Anschutz, A.J., Smolen, J.M., Simcik, M.F., Penn, R.L., 2007. The adsorption of perfluorooctane sulfonate onto sand, clay, and iron oxide surfaces. J Chem Eng Data 52, 1165-1170.

Kärrman, A., Bjurlid, F., Hagberg, J., Ricklund, N., Larsson, M., Stubleski, J., Hollert, H., 2016. Study of environmental and human health impacts of firefighting agents (technical report). MTM Research Centre, Örebro University.

Kärrman, A., Elgh-Dalgren, K., Lafossas, C., Moskeland, T., 2011. Environmental levels and distribution of structural isomers of perfluoroalkyl acids after aqueous fire-fighting foam (AFFF) contamination. Environ Chem 8, 372-380.

Kauck, E.A., Diesslin, A.R., 1951. Some Properties of Perfluorocarboxylic Acids. Ind Eng Chem 43, 2332-2334.

KEMI, 2015. The Swedish Chemicals Agency: Chemical Analysis of Selected Fire-fighting Foams on the Swedish Market 2014 PM 6/15

Kerger, B.D., Copeland, T.L., DeCaprio, A.P., 2011. Tenuous dose-response correlations for common disease states: case study of cholesterol and perfluorooctanoate/sulfonate (PFOA/PFOS) in the C8 Health Project. Drug Chem Toxicol 34, 396-404.

Kissa, E., 2001. Fluorinated Surfactants and Repellents.

Kleiner, E., Jho, C., 2009. Recent developments in 6: 2 fluorotelomer surfactants and foam stabilizers. 4th Reebok Foam Seminar, pp. 6-7.

Krabbenhoft, D., Bowser, C.J., Anderson, M.P., Valley, J.W., 1990. Estimating groundwater exchange with lakes: 1. The stable isotope mass balance method. Water Resour Res 26, 2245-2453.

Kucharzyk, K.H., Darlington, R., Benotti, M., Deeb, R., Hawley, E., 2017. Novel treatment technologies for PFAS compounds: A critical review. J Environ Manag 204, 757-764.

Kwadijk, C.J.A.F., Kotterman, M., Koelmans, A.A., 2014. Partitioning of Perfluorooctanesulfonate and Perfluorohexanesulfonate in the Aquatic Environment after an Accidental Release of Aqueous Film Forming Foam at Schiphol Amsterdam Airport. Environ Toxicol Chem 33, 1761-1765.

Levine, A.D., Libelo, E., Bugna, G., Shelley, T., Mayfield, H., Stauffer, T., 1998. Biogeochemical assessment of natural attenuation of JP-4 contaminated ground water in the presence of fluorinated surfactants. Sci Total Environ 208, 179-195.

Li, Y., Barregard, L., Xu, Y., Scott, K., Pineda, D., Lindh, C.H., Jakobsson, K., Fletcher, T., 2020. Associations between perfluoroalkyl substances and serum lipids in a Swedish adult population with contaminated drinking water. Environ Health 19, 33.

Livsmedelsverket, 2021. Livsmedelsverket (Swedish Food Agency): Riskhantering PFAS i dricksvatten och egenfångad fisk, web source: https://www.livsmedelsverket.se/ produktion-handel--kontroll/dricksvattenproduktion /riskhantering-pfas-i-dricksvatten-egenfangad-fisk (accessed on 2021-09-02).

Mastrantonio, M., Bai, E., Uccelli, R., Cordiano, V., Screpanti, A., Crosignani, P., 2018. Drinking water contamination from perfluoroalkyl substances (PFAS): an ecological mortality study in the Veneto Region, Italy. Eur J Public Health 28, 180-185.

McCarthy, C., Kappleman, W., DiGuiseppi, W., 2017a. Ecological Considerations of Per- and Polyfluoroalkyl Substances (PFAS). Curr Pollut Rep 3, 289-301.

McCarthy, C., Kappleman, W., DiGuiseppi, W., 2017b. Ecological Considerations of Per- and Polyfluoroalkyl Substances (PFAS). Curr Pollut Rep 3, 289-301.

Merino, N., Qu, Y., Deeb, R.A., Hawley, E.L., Hoffmann, M.R., Mahendra, S., 2016. Degradation and Removal Methods for Perfluoroalkyl and Polyfluoroalkyl Substances in Water. Environ Eng Sci 33, 615-649.

Moody, C., Field, J.A., 1999. Determination of Perfluorocarboxylates in Groundwater Impacted by Fire-Fighting Activity. Environ Sci Technol 33.

Moody, C.A., Field, J.A., 2000. Perfluorinated surfactants and the environmental implications of their use in fire-fighting foams. Environ Sci Technol 34, 3864-3870.

Moody, C.A., Hebert, G.N., Strauss, S.H., Field, J.A., 2003. Occurrence and persistence of perfluorooctanesulfonate and other perfluorinated surfactants in groundwater at a fire-training area at Wurtsmith Air Force Base, Michigan, USA. J Environ Monitor 5, 341-345.

Moody, C.A., Martin, J.W., Kwan, W.C., Muir, D.C.G., Mabury, S.C., 2002. Monitoring perfluorinated surfactants in biota and surface water samples following an accidental release of fire-fighting foam into Etobicoke Creek. Environ Sci Technol 36, 545-551.

Murray, C.C., Vatankhah, H., McDonough, C.A., Nickerson, A., Hedtke, T.T., Cath, T.Y., Higgins, C.P., Bellona, C.L., 2019. Removal of per- and polyfluoroalkyl substances using super-fine powder activated carbon and ceramic membrane filtration. J Hazard Mater 366, 160-168.

Nouhi, S., Ahrens, L., Pereira, H.C., Hughes, A.V., Campana, M., Gutfreund, P., Palsson, G.K., Vorobiev, A., Hellsing, M.S., 2018. Interactions of perfluoroalkyl substances with a phospholipid bilayer studied by neutron reflectometry. J Colloid Interf Sci 511, 474-481.

Oberg, M., Da Silva, A., Ringblom, J., Scott, K., Lindh, C., Jakobsson, K., 2018. Probabilistic risk of decreased levels of triiodothyronine following chronic exposure to PFOS and PFHxS. Toxicol Lett 295, S224-S224.

Ochiai, T., Iizuka, Y., Nakata, K., Murakami, T., Tryk, D.A., Fujishima, A., Koide, Y., Morito, Y., 2011a. Efficient electrochemical decomposition of perfluorocarboxylic acids by the use of a boron-doped diamond electrode. Diam Relat Mater 20, 64-67.

Ochiai, T., Iizuka, Y., Nakata, K., Murakami, T., Tryk, D.A., Koide, Y., Morito, Y., Fujishima, A., 2011b. Efficient Decomposition of Perfluorocarboxylic Acids in Aqueous Suspensions of a TiO2 Photocatalyst with Medium-Pressure Ultraviolet Lamp Irradiation under Atmospheric Pressure. Ind Eng Chem Res 50, 10943-10947.

Ochiai, T., Moriyama, H., Nakata, K., Murakami, T., Koide, Y., Fujishima, A., 2011c. Electrochemical and Photocatalytic Decomposition of Perfluorooctanoic Acid with a Hybrid Reactor Using a Boron-doped Diamond Electrode and TiO2 Photocatalyst. Chem Lett 40, 682-683.

Ochoa-Herrera, V., Sierra-Alvarez, R., Somogyi, A., Jacobsen, N.E., Wysocki, V.H., Field, J.A., 2008. Reductive defluorination of perfluorooctane sulfonate. Environ Sci Technol 42, 3260-3264.

Paul, A.G., Jones, K.C., Sweetman, A.J., 2009. A First Global Production, Emission, And Environmental Inventory For Perfluorooctane Sulfonate. Environ Sci Technol 43, 386-392.

Pereira, H.C., Ullberg, M., Kleja, D.B., Gustafsson, J.P., Ahrens, L., 2018. Sorption of perfluoroalkyl substances (PFASs) to an organic soil horizon - Effect of cation composition and pH. Chemosphere 207, 183-191.

Pistocchi, A.L., R., 2009. A Map of European Emissions and Concentrations of PFOS and PFOA. Environ Sci Technol 43, 9237-9244.

Place, B.J., Field, J.A., 2012. Identification of Novel Fluorochemicals in Aqueous Film-Forming Foams Used by the US Military. Environ Sci Technol 46, 7120-7127.

Powley, C.R., George, S.W., Ryan, T.W., Buck, R.C., 2005. Matrix effect-free analytical methods for determination of perfluorinated carboxylic acids in environmental matrixes. Anal Chem 77, 6353-6358.

Prevedouros, K., Cousins, I.T., Buck, R.C., Korzeniowski, S.H., Buck, R.C., Korzeniowski, S.H., 2006. Sources, fate and transport of perfluorocarboxylates. Environ Sci Technol 40, 32-44.

Quinones, O., Snyder, S.A., 2009. Occurrence of Perfluoroalkyl Carboxylates and Sulfonates in Drinking Water Utilities and Related Waters from the United States. Environ Sci Technol 43, 9089-9095.

Rahman, M.F., Peldszus, S., Anderson, W.B., 2014. Behaviour and fate of perfluoroalkyl and polyfluoroalkyl substances (PFASs) in drinking water treatment: A review. Water Res 50, 318-340.

Rayne, S., Forest, K., 2009. Perfluoroalkyl sulfonic and carboxylic acids: A critical review of physicochemical properties, levels and patterns in waters and wastewaters, and treatment methods. J Environ Sci Health A Tox Hazard Subst Environ Eng 44, 1145-1199.

Reagen, W.K., Lindstrom, K.R., Jacoby, C.B., Purcell, R.G., Kestner, T.A., Payfer, R.M., 2007. Environmental characterization of 3M electrochemical fluorination derived perfluorooctanoate and perfluorooctanesulfonate. SETAC North American 28th Annual Meeting in Milwaukee U.S, 1-33.

Remucal, C.K., 2019. Spatial and temporal variability of perfluoroalkyl substances in the Laurentian Great Lakes. Environ Sci-Proc Imp 21, 1816-1834.

Rupert, W., Verdonik, D., Hanauska, C., 2005. Environmental Impacts of Fire Fighting Foams. Hughes Associates, Inc.

Ryota, S., 2019. Kyoto University professors detect PFOS concentration of 4 times national average in Ginowan residents' blood. Ryukyu Shimpo, 17 May 2019. Available online: http://english.ryukyushimpo.jp/2019/05/21/30452/ (accessed on 15 June 2020).

Sacks, L.A., Swancar, A., Lee, T.M., 1998. Estimating Ground-Water Exchange with Lakes Using Water-Budget and Chemical Mass-Balance Approaches for Ten Lakes in Ridge Areas of Polk and Highlands Counties, Florida. Water-Resources Investigations. USGS.

Sakurai, T., Serizawa, S., Isobe, T., Kobayashi, J., Kodama, K., Kume, G., Lee, J.H., Maki, H., Imaizumi, Y., Suzuki, N., Horiguchi, T., Morita, M., Shiraishi, H., 2010. Spatial, Phase, And Temporal Distributions of Perfluorooctane Sulfonate (PFOS) and Perfluorooctanoate (PFOA) in Tokyo Bay, Japan. Environ Sci Technol 44, 4110-4115.

Sanchez-Cabeza, J.A., Ani-Ragolta, I., Masque, P., 2000. Some considerations of the Pb-210 constant rate of supply (CRS) dating model. Limnol Oceanogr 45, 990-995.

Schaefer, C.E., Andaya, C., Burant, A., Condee, C.W., Urtiaga, A., Strathmann, T.J., Higgins, C.P., 2017. Electrochemical treatment of perfluorooctanoic acid and perfluorooctane sulfonate: Insights into mechanisms and application to groundwater treatment. Chem Eng J 317, 424-432.

Schaefer, C.E., Andaya, C., Urtiaga, A., McKenzie, E.R., Higgins, C.P., 2015. Electrochemical treatment of perfluorooctanoic acid (PFOA) and perfluorooctane sulfonic acid (PFOS) in groundwater impacted by aqueous film forming foams (AFFFs). J Hazard Mater 295, 170-175.

Schroder, H.F., 2003. Determination of fluorinated surfactants and their metabolites in sewage sludge samples by liquid chromatography with mass spectrometry and tandem mass spectrometry after pressurised liquid extraction and separation on fluorine-modified reversed-phase sorbents. J Chromatogr A 1020, 131-151.

Schroder, H.F., Meesters, R.J.W., 2005. Stability of fluorinated surfactants in advanced oxidation processes - A follow up of degradation products using flow injection-mass spectrometry, liquid chromatography-mass spectrometry and liquid chromatography-multiple stage mass spectrometry. J Chromatogr A 1082, 110-119.

Schultz, M.M., Barofsky, D.F., Field, J.A., 2004. Quantitative determination of fluorotelomer sulfonates in groundwater by LC MS/MS. Environ Sci Technol 38, 1828-1835.

Shin, H.M., Steenland, K., Ryan, P.B., Vieira, V.M., Bartell, S.M., 2014. Biomarker-Based Calibration of Retrospective Exposure Predictions of Perfluorooctanoic Acid. Environ Sci Technol 48, 5636-5642.

Shin, H.M., Vieira, V.M., Ryan, P.B., Steenland, K., Bartell, S.M., 2013. Retrospective Exposure Estimation and Predicted versus Observed Serum Perfluorooctanoic Acid Concentrations for Participants in the C8 Health Project (vol 119, pg 1760, 2011). Environ Health Persp 121, A113-A113.

Shinoda, K., Hato, M., Hayashi, T., 1972. Physicochemical properties of aqueous solutions of fluorinated surfactants. J Phys Chem 76.

Sinclair, E., Kannan, K., 2006. Mass loading and fate of perfluoroalkyl surfactants in wastewater treatment plants. Environ Sci Technol 40, 1408-1414.

SMHI, 2019. Normal uppmätt årsnederbörd, medelvärde 1961-1990. Swedish Meteorological and Hydrological Institute.

Soriano, A., Gorri, D., Urtiaga, A., 2017. Efficient treatment of perfluorohexanoic acid by nanofiltration followed by electrochemical degradation of the NF concentrate. Water Res 112, 147-156.

Swarzenski, P.W., 2013. 210Pb Dating. Encyclopedia of Scientific Dating Methods, 1-11.

Taniyasu, S., Kannan, K., Horii, Y., Hanari, N., Yamashita, N., 2003. A survey of perfluorooctane sulfonate and related perfluorinated organic compounds in water, fish, birds, and humans from Japan. Environ Sci Technol 37, 2634-2639.

Taniyasu, S., Kannan, K., So, M.K., Gulkowska, A., Sinclair, E., Okazawa, T., Yamashita, N., 2005. Analysis of fluorotelomer alcohols, fluorotelorner acids, and short- and long-chain perfluorinated acids in water and biota. J Chromatogr A 1093, 89-97.

Trautmann, A.M., Schell, H., Schmidt, K.R., Mangold, K.M., Tiehm, A., 2015. Electrochemical degradation of perfluoroalkyl and polyfluoroalkyl substances (PFASs) in groundwater. Water Sci Technol 71, 1569-1575.

Turekova, I., Karol, B., 2010. The Environmental Impacts of Fire-Fighting Foams. Research Papers Faculty of Materials Science and Technology Slovak University of Technology 18, 111-120.

Vecitis, C.D., Park, H., Cheng, J., Mader, B.T., Hoffmann, M.R., 2008a. Enhancement of Perfluorooctanoate and Perfluorooctanesulfonate Activity at Acoustic Cavitation Bubble Interfaces. J Phys Chem C 112, 16850-16857.

Vecitis, C.D., Park, H., Cheng, J., Mader, B.T., Hoffmann, M.R., 2008b. Kinetics and mechanism of the sonolytic conversion of the aqueous perfluorinated surfactants, perfluorooctanoate (PFOA), and perfluorooctane sulfonate (PFOS) into inorganic products. J Phys Chem A 112, 4261-4270.

Vecitis, C.D., Wang, Y., Cheng, J., Park, H., Mader, B.T., Hoffmann, M.R., 2010. Sonochemical Degradation of Perfluorooctanesulfonate in Aqueous Film-Forming Foams. Environ Sci Technol 44, 432-438.

Weber, A.K., Barber, L.B., LeBlanc, D.R., Sunderland, E.M., Vecitis, C.D., 2017. Geochemical and Hydrologic Factors Controlling Subsurface Transport of Poly- and Perfluoroalkyl Substances, Cape Cod, Massachusetts. Environ Sci Technol 51, 4269-4279.

Weiss, O., Wiesmuller, G.A., Bunte, A., Coen, T., Schmidt, C.K., Wilhelm, M., Holzer, J., 2012. Perfluorinated compounds in the vicinity of a fire training area - Human biomonitoring among 10 persons drinking water from contaminated private wells in Cologne, Germany. Int J Hyg Envir Heal 215, 212-215.

Xiao, F., 2015. Comment on "Perfluorooctanoic acid (PFOA) and perfluorooctanesulfonic acid (PFOS) in surface waters, sediments, soils and wastewater - A review on concentrations and distribution coefficients" by Zareitalabad et al. [Chemosphere 91(6) (2013) 725-732]. Chemosphere 138, 1056-1057.

Zareitalabad, P., Siemens, J., Hamer, M., Amelung, W., 2013. Perfluorooctanoic acid (PFOA) and perfluorooctanesulfonic acid (PFOS) in surface waters, sediments, soils and wastewater - A review on concentrations and distribution coefficients. Chemosphere 91, 725-732.